uninfected H9 cells. The cells harvested at each passage were subjected to PCR for amplification of HIV-1 *gag* region and direct DNA sequencing was performed. The viral populational changes were determined by relative peak height on sequence electrophoregram (Kosalaraksa et al., 1999).

### 2.5. HIV-1 susceptibility to NFV

MT-2 cells were infected with 500 $TCID_{50}$ of each virus in the absence and the presence of 0.001, 0.00316, 0.01, 0.0316, 0.1, 0.316, 1, and 3.16 μM of NFV, and cultured in triplicate for 7 days. At the end of culture, the amounts of p24 in the supernatants were measured and 50% inhibitory concentrations ($IC_{50}$) of NFV were determined by referring to the dose–response curve.

### 2.6. Western blot analysis of HIV-1 virions

HeLa cells were transfected with pNL4-3 and *gag*-protease recombinant HIV-1 plasmid DNA in the absence and presence of 0.1 μM NFV. The culture supernatant was harvested at 48 h after transfection, centrifuged at 37,000 × *g* for 90 min to pellet virus particles. The virion pellet ($6 \times 10^5$ cpm of RT activity) was applied to an SDS gradient gel electrophoresis and transferred to a nitrocellulose membrane. The membrane was incubated with anti-HIV-1 p24 antisera (Advanced Biotechnology, Columbia, USA) and HIV-1-infected patients' serum, respectively, and hybridized with anti-protein A antibody conjugated with horseradish peroxidase (Amersham Pharmacia Biotech, Uppsala, Sweden). The immune complex was visualized with an ECL Plus system (Amersham Pharmacia Biotech) according to the manufactures' description.

The percent signal density of Gag products was analyzed on a Windows computer by using the ImageJ Program (developed at the U.S. National Institutes of Health (http://www.rsb.info.nih.gov/ij/)) and the percent density of p24 was determined by the following formula: percent density of p24 = 100 × (the density of p24 signal)/(the cumulated density of all *Gag* signals) (Tamiya et al., 2004).

## 3. Results

### 3.1. Whole capsid substitutions necessary for NFV-enhanced replication

MAmt, carrying only the substitutions in the matrix (Fig. 2), grew well in the absence of NFV (Fig. 3). In the presence of NFV, however, it did not grow at all, indicating that matrix substitutions were not sufficient to confer NFV resistance. MA + PRmt, carrying substitutions in the matrix and protease (Fig. 2), replicated as efficiently as PRmt (carrying only the substitutions in protease), both in the absence and presence of 0.1 μM NFV, though its replication was not enhanced with NFV, indicating that the substitutions in matrix and protease were not sufficient for NFV-dependent enhancement of replication. As reported in our previous study (Matsuoka-Aizawa et al., 2003), p17PRmt replicated more efficiently in the presence of 0.1 μM NFV than in the absence of NFV. Therefore, some of the substitutions in the capsid should be responsible for such unique phenotype of CL-4 strain. The HIV-1 capsid contains two domains, a C-terminal oligomerization domain and N-terminal core domain, which function differently in viral assembly (Turner and Summers, 1999). Therefore, we divided the EcoT22I—ApaI segment of CL-4 into two segments at ACC I site, named them the N-terminal half of the capsid (NCA) and the C-terminal half of the capsid (CCA), and constructed two recombinant HIV-1 clones, NCAmt and CCAmt, which possessed all the substitutions in the matrix and protease of CL-4, and the substitutions in NCA and CCA, respectively (Fig. 2). NCAmt and CCAmt grew efficiently both in the absence and presence of 0.1 μM NFV, and only NCAmt showed weak replication enhancement with 0.1 μM NFV in PM-1 and MT-2 cells though it was not so efficient as that of p17PRmt, suggesting that the substitutions in CCA, contributed to the efficient replication enhancement of p17PRmt (Fig. 3). CCAmt did not show the p17PRmt's phenotype, indicating that the substitutions in NCA were indispensable for replication enhancement. As we reported previously (Matsuoka-Aizawa et al., 2003), p24PRmt lacking the substitutions in matrix did not show replication enhancement by NFV. Taken together, the substitutions in the whole matrix, capsid, SP1, and the N-terminal end of nucleocapsid of CL-4 were indispensable for efficient replication enhancement of p17PRmt.

To define further the role of substitutions in the matrix, NCA, and CCA, viral replication efficiency was compared among the HIV-1 clones described above in the absence and presence of NFV using competitive HIV-1 replication assay (Kosalaraksa et al., 1999). MA + PRmt outgrew PRmt both in the absence and presence of 0.1 μM NFV (Fig. 4a), and MAmt was outgrown by NL4-3 in the absence of NFV (Fig. 4b), suggesting that the substitutions in the matrix of CL-4 reduced the replication of HIV-1 harboring wild-type protease, but compensated the replication of HIV-1 harboring NFV-resistant protease of CL-4. NCAmt outgrew MA + PRmt both in the absence and presence of 0.1 μM NFV (Fig. 4c), suggesting that the substitutions in NCA were compensatory for the replication of HIV-1 harboring protease and matrix of CL-4. However, CCAmt was outgrown by MA + PRmt in the absence of NFV, but its replication in the presence of 0.1 μM NFV was comparable with that of MA + PRmt under similar condition (Fig. 4d), suggesting that the substitutions in CCA reduced the replication capability of MA + PRmt, while NFV compensated the mutation effect. Sub-cloning analyses of proviral sequences at both of the passages 3 and 4 in competitive HIV-1 replication assay in the presence of 0.1 μM NFV showed that five of 10 clones were derived from CCAmt and the other five clones were derived from MA + PRmt, which confirmed that CCAmt and MA + PRmt had comparable replication ability in the presence of 0.1 μM NFV (Fig. 4d). MA + PRmt readily outgrew p17PRmt in the absence of NFV, but was outgrown by p17PR in the presence of 0.1 μM NFV (Fig. 4e), suggesting that the substitutions in NCA and CCA reduced the replication capability of MA + PRmt, while NFV counteracted the mutation effect and rather enhanced replication ability at sub-inhibitory concentration (Fig. 3, p17PRmt).

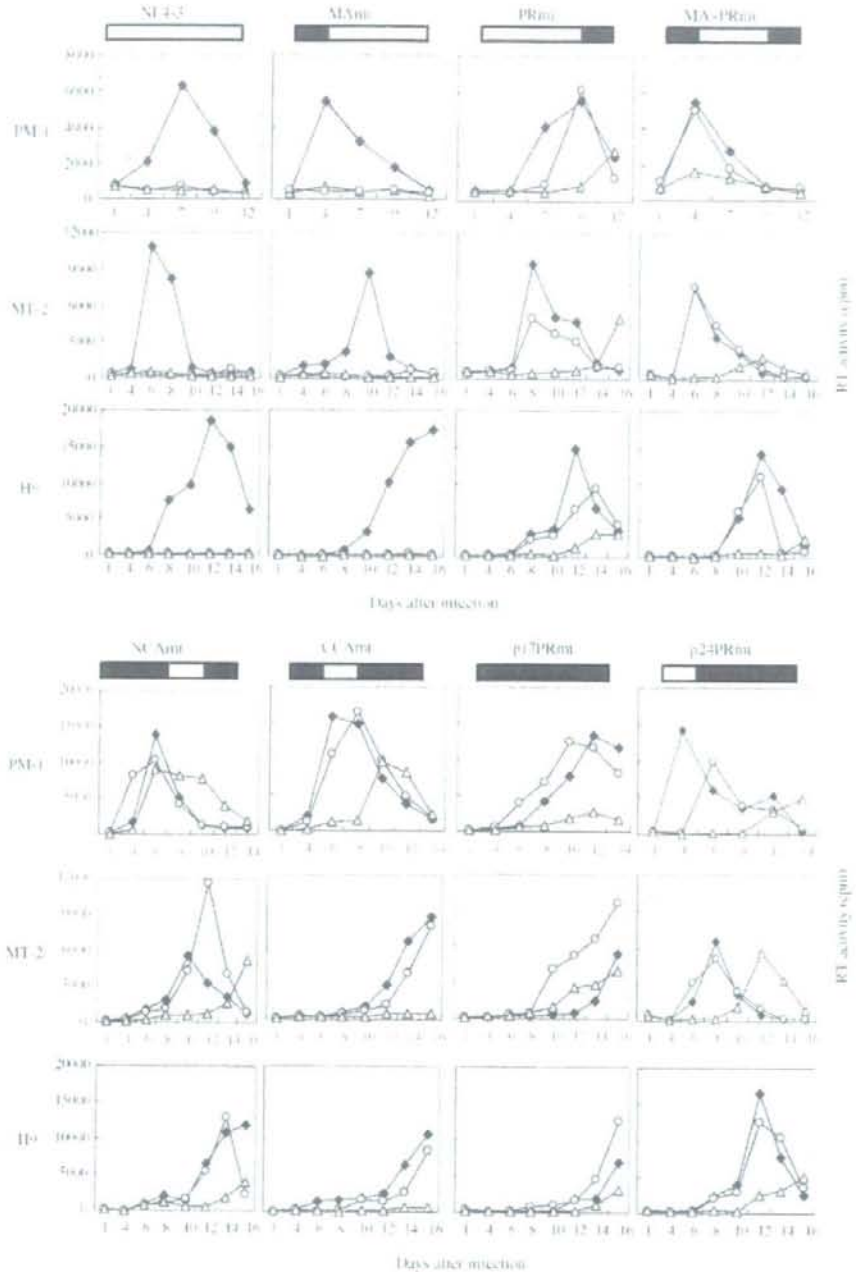


Fig. 3. Effects of NFV on replication capability of recombinant HIV-1s. PM-1, MT-2, and H9 cells ($2 \times 10^4$ cells) were exposed to 0.2 ml of cell-free supernatant containing each HIV-1 clone ($2 \times 10^5$ $^{32}$P cpm of RT activity), washed once, and cultured in 0.2 ml of medium in the absence (closed diamonds) and presence of NFV (0.1 μM; open circles, 1 μM; open triangles). Half volume of the culture medium was changed every 2 or 3 days, and the supernatant was kept at −80 °C until the measurement of RT activity. Each experiment was carried out in duplicate and repeated three times, and representative data are shown.

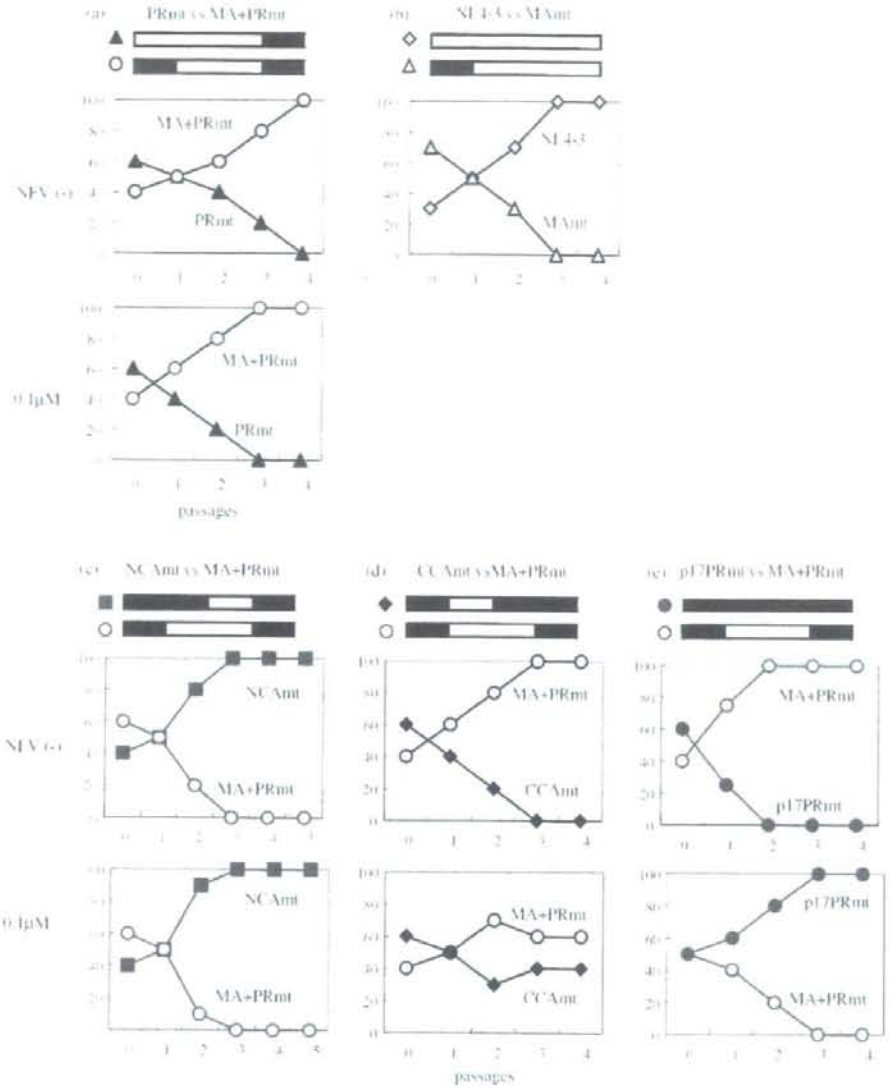


Fig. 4. One-to-one competitive HIV-1 replication assay. H9 cells ($2 \times 10^5$ cells) were incubated with two recombinant HIV-1s (each of 100 $TCID_{50}$) simultaneously at 37 °C for 16 h, washed with PBS twice, and cultured in the absence and presence of 0.1 μM of NFV. At 7 days post-infection, the culture supernatant was used to infect fresh uninfected H9 cells. The cells harvested at each passage were subjected to direct DNA sequencing, and the viral population changes were determined by the relative peak height in the sequencing electrophoregram. The persistence of the original amino acid substitutions was confirmed for all infectious clones used in this assay. (a) PRmt vs. MA + PRmt; (b) NL4-3 vs. MAmt; (c) NCAmt vs. MA + PRmt; (d) CCAmt vs. MA + PRmt; (e) p17PRmt vs. MA + PRmt.

### 3.2. Gag substitutions conferring NFV resistance

To analyze the role of the substitutions in the matrix, NCA, and CCA in NFV resistance, $IC_{50}$s of NFV for the HIV-1 clones described above were determined by using MT-2 cells (Zhang et al., 1997). MAmt ($IC_{50}$: 9.4 nM) showed 1.9-fold resistance against NFV compared with NL4-3 (5.0 nM), and p17PRmt (893 nM) showed 3.3-fold resistance compared with p24PRmt (273 nM) (Table 1), indicating that the substitutions in the matrix may make a small contribution to the viral resistance against NFV. NCAmt (483 nM) had 2.1-fold resistance against NFV compared with MA + PRmt (229 nM), and p17PRmt had 4.1-fold resistance compared with CCAmt (217 nM), indicating that the substitutions in NCA gave positive impact on viral resistance. Interestingly, CCAmt showed 0.95-fold resistance against NFV compared with MA + PRmt, indicating that substitutions in CCA

Table 1
NFV resistance of recombinant HIV-1s

| HIV-1 | $IC_{50}$ (nM) | Fold-resistance |
|---|---|---|
| NL4-3 | 5.0 ± 0.4 | 1.0 |
| PRmt | 241 ± 34 | 48 |
| p24PRmt | 273 ± 13 | 55 |
| p17PRmt | 893 ± 28 | 179 |
| MAmt | 9.4 ± 3.3 | 1.9 |
| MA + PRmt | 229 ± 21 | 46 |
| NCAmt | 483 ± 26 | 97 |
| CCAmt | 217 ± 32 | 43 |

The concentrations of drug added to the growth medium for calculation of the $IC_{50}$s were 0, 1, 3.16, 10, 31.6, 100, and 316 nM and 1 and 3.16 μM NFV, and the $IC_{50}$s were derived from plots of percent of inhibition of p24 production in culture supernatant versus NFV concentration.

may give small negative impact on viral resistance in the absence of the substitutions in NCA. p17PRmt, however, had 1.8-fold resistance compared with NCAmt, indicating the substitutions in CCA may give a small but positive contribution to viral resistance in the presence of the substitutions in NCA. The role of the substitutions in CCA in viral resistance was altered by the presence of the substitutions in NCA.

### *3.3. Gag substitutions facilitating cleavage between matrix and capsid*

To further delineate the impact of each substitution, the Gag processing pattern was assessed in the absence and presence of NFV by Western blot analysis using anti-p24 monoclonal antibody (Fig. 5A1–2 and B1–2). As expected, 0.1 μM of NFV effectively blocked cleavage of the Gag p55 precursor of NL4-3 (percent density of p24; 4.7% versus 87.5% in Fig. 5A1; 4.2% versus 83.3% in Fig. 5A2). In contrast, NFV gave only a small influence on the cleavage patterns of the p55 precursor of MA + PRmt (percent density of p24; 65.5% versus 87.4% in Fig. 5A1; 77.8% versus 92.6% in Fig. 5A2), which is consistent with the indistinguishable replication kinetics of this mutant in the absence and presence of NFV (Fig. 3). Interestingly, NFV enhanced the cleavability of the p55 precursor of p17PRmt (percent density of p24; 94.8% versus 74.3% in Fig. 5A1; 72.2% versus 54.1% in Fig. 5A2), which was paralleled with NFV-dependent replication enhancement of this mutant (Fig. 3). NFV also gave a small positive effect on the cleavability of the p55 precursor of NCAmt (percent density of p24; 97.1% versus 94.6% in Fig. 5B1; 97.5% versus 96.2% in Fig. 5B2), which was paralleled with the partial enhancement of replication with NFV (Fig. 3). Furthermore, percent density of p24 of NCAmt was increased compared with that of MA + PRmt (percent density of p24; 94.6% and 96.2% versus 87.4% and 92.6% in the absence of NFV; 97.1% and 97.5% versus 65.5% and 77.8% in the presence of 0.1 μM NFV), suggesting that the substitutions in NCA play a significant role in Gag cleavability. Finally, NFV decreased percent density of p24 of CCAmt (percent density of p24; 68.9% versus 78.2% in Fig. 5B1; 45.3% versus 79.0% in Fig. 5B2), which was paralleled with NFV-induced delay of replication kinetics (Fig. 3). For further confirmation, the Gag processing pattern of NCAmt and CCAmt was also assessed by Western blot analysis using HIV-1-infected patient's serum (Fig. 5B3). As expected, NFV slightly increased cleavability of the p55 precursor of NCAmt (percent density of p24; 96.9% versus 94.5% in Fig. 5B3), and gave a negative impact on Gag cleavage of CCAmt (percent density of p24; 41.9% versus 74.3% in Fig. 5B3), which were well compatible with the cleavage pattern analyzed by using anti-p24 monoclonal antibody (Fig. 5B1, 2). In summary, NFV induced enhanced cleavability of Gag precursors of p17PRmt and NCAmt, which was well paralleled with NFV-induced enhancement of replication capability of these mutants.

## 4. Discussion

We previously reported that the substitutions in p6-protease segment alone are sufficient to confer NFV resistance while those in matrix are indispensable for the replication enhancement of CL-4 by NFV (Matsuoka-Aizawa et al., 2003). In the present study, we found that not only the matrix substitutions but the mutations in N-terminal half of capsid also played critical role in the enhancement and that the full potential of the enhancement phenotype was achieved only with the cooperation of mutations in the entire Gag and protease region of CL-4. The substitutions in matrix and those in N-terminal half of capsid compensated the otherwise compromised viral replication in the absence and presence of NFV (Fig. 4a and c). Probably, these substitutions cooperatively altered the tertiary structure of the Gag precursor and made the cleavage site between matrix and capsid more accessible to mutant protease harboring multiple resistance-associated mutations. The cleavage pattern analyzed by Western blot analysis supported the idea that the substitutions in N-terminal half of capsid improved the Gag cleavage. Percent density of p24 of NCAmt was increased compared with that of MA + PRmt in the absence of NFV (Fig. 5A1–2 and B1–2; 94.6% and 96.2% versus 87.4% and 92.6%). It is worth noting that CL-4 had a total of 56 amino acid substitutions in *gag-pro* genes compared with NL4-3; 22 substitutions had emerged during NFV-containing therapy, and 34 other substitutions had already existed before the introduction of the therapy, and that all the substitutions in N-terminal half of capsid of CL-4 were pre-existing before NFV-therapy (Fig. 1), suggesting that certain polymorphic amino acid residues seen in HIV-1 clinical isolates were associated with drug resistance. Interestingly, the amino acid insertion at the same site of the matrix of CL-4 compared with NL4-3 (Fig. 1; amino acids 121–125 in MA, QQAAA) was reported to increase viral replication harboring mutant protease by improving otherwise impaired Gag processing (Tamiya et al., 2004). Gatanaga et al. also reported that a polymorphic substitution in N-terminal half of capsid was indispensable for the development of high multitude of resistance against PIs (Gatanaga et al., 2002), though CL-4 did not harbor the same substitution. It is also known that certain drug-resistance-conferring amino acid substitutions found in one subtype HIV-1 isolated from patients under therapy may be detected in HIV-1 of other subtypes from untreated individuals (Cornelissen et al., 1997; Quinones-Mateu et al., 1998). More-

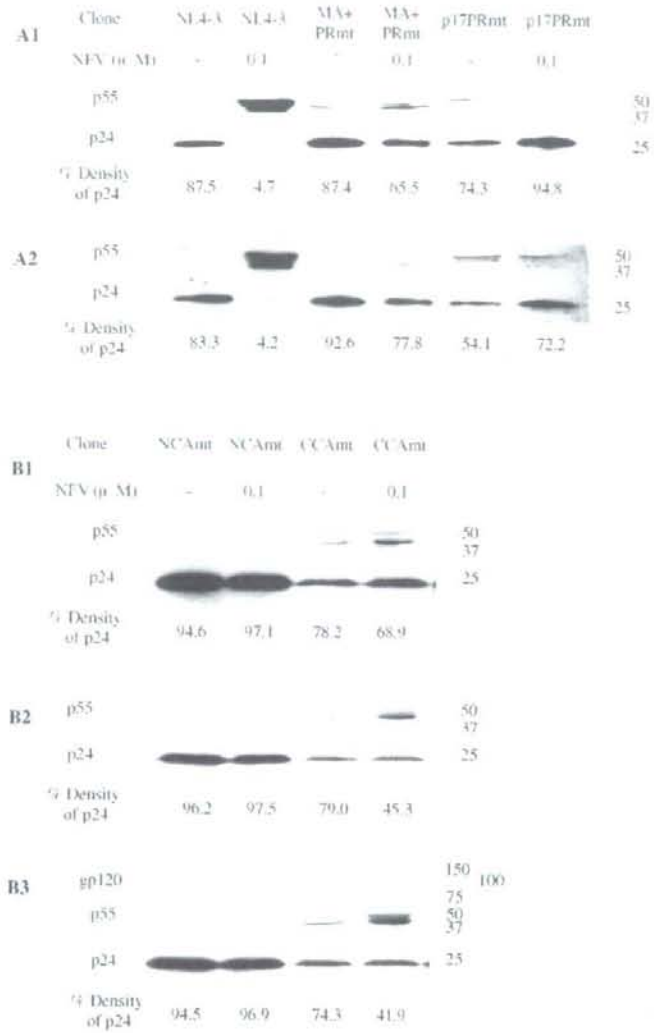


Fig. 5. Western blot analysis in the absence and presence of NFV. HeLa cells were transfected with each of full-length molecular clones and cultured in the absence and presence of 0.1 μM NFV. At 48 h post-transfection, virions in the culture supernatant ($6 \times 10^5$ cpm of RT activity) were harvested and subjected to Western blot analysis. Gag proteins were visualized by using anti-p24 monoclonal antibody (A1-2, B1-2) and HIV-1-infected patient's serum (B3). Percent density of p24 was calculated as 100 × (p24 signal density/total Gag product signal densities) in a Western blot.

over, a recent study of Colson et al. revealed that HIV-2 strains harbor specific patterns of natural polymorphism and resistance (Colson et al., 2004). HIVs seem to acquire drug-resistance by utilizing the pre-existing polymorphic mutations and by coordinating the development of multiple substitutions.

Furthermore, the substitutions in N-terminal half of capsid of CL-4 altered the effect of NFV on viral replication. Sub-inhibitory concentration (0.1 μM) of NFV slightly accelerated the Gag precursor cleavage of NCAmt (percent density of p24; 97.1% versus 94.6% in Fig. 5B1; 97.5% versus 96.2% in Fig. 5B2; 96.9% versus 94.5% in Fig. 5B3), which was paralleled with the partial replication enhancement with NFV (Fig. 3), though it showed inhibitory effect in Gag processing of MA + PRmt (percent density of p24; 65.5% versus 87.4% in Fig. 5A1; 77.8% versus 92.6% in Fig. 5A2). Therefore, one of the mechanisms of viral replication enhancement with NFV is the improved processing of Gag harboring the substitutions in N-terminal half of capsid of CL-4 cooperated with the substitutions in the matrix. On the other hand, the role of the substitutions in C-terminal half of capsid seemed different, though they were also indispensable for the full potential of replication enhancement with NFV. They impaired the cleavability of Gag precursor

of MA + PRmt (Fig. 5A1–2 and B1–2; percent density of p24; CCAmt versus MA + PRmt = 78.2% and 79.0% versus 87.4% and 92.6%) and NCAmt (Fig. 5A1–2 and B1–2; percent density of p24; p17PRmt versus NCAmt = 74.3% and 54.1% versus 94.6% and 96.2%) in the absence of NFV, which were parallel with viral replication data (CCAmt versus MA + PRmt, Fig. 4d; p17PRmt versus NCAmt, Fig. 3). The effects of NFV on Gag cleavage pattern were different between CCAmt and p17PRmt; sub-inhibitory concentration (0.1 μM) of NFV facilitated the Gag cleavability of p17PRmt (percent density of p24; 94.8% versus 74.3% in Fig. 5A1; 72.2% versus 54.1% in Fig. 5A2), though it decreased the cleavability of CCAmt Gag (percent density of p24; 68.9% versus 78.2% in Fig. 5B1; 45.3% versus 79.0% in Fig. 5B2; 41.9% versus 74.3% in Fig. 5B3), which was also parallel with viral replication data showing enhancement only in p17PRmt but not in CCAmt (Fig. 3). Considering together, the substitutions in C-terminal half of capsid compromised viral replication by impairing the Gag preprocessing, and NFV could counteract the negative impact only in the presence of the substitutions in N-terminal half of capsid. In the absence of the substitutions in N-terminal half of capsid, only partial counteraction was seen (Fig. 4d). In summary, NFV-induced viral replication enhancement of CL-4 was caused by two mechanisms; NFV facilitates the processing of Gag harboring the substitutions in the matrix and N-terminal half of capsid of CL-4, and NFV counteracts the impaired Gag cleavage caused by the substitutions in C-terminal half of capsid of CL-4 only in the presence of the substitutions in the matrix and N-terminal half of capsid of CL-4. Therefore, the full potential of the enhancement phenotype was achieved only with the cooperation of mutations in the entire Gag and protease region of CL-4.

Notably, we found several other PI-resistant isolates with the phenotype of PI-dependent replication enhancement (data not shown), suggesting that HIV-1 can evolve to acquire capability to replicate better with the drugs. Such replication enhancement with antiretroviral agents presents formidable challenge in the therapy of HIV-1 infection. Future studies of structural analyses of Gag precursor(s) harboring substitutions of these mutants are warranted to clarify the underlying mechanism(s).

## Acknowledgments

The authors thank A. Hachiya, K. Tsuchiya, Y. Suzuki, and Y. Hirabayashi for their helpful suggestions and continuous discussions throughout this study. We are also indebted to Y. Takahashi and F. Negishi for their technical assistance. This study was supported by a Grant-in-Aid for AIDS Research from the Ministry of Health, Labor, and Welfare of Japan (H15-AIDS-001), by the Organization of Pharmaceutical Safety and Research (01-4), and by the Japanese Foundation for AIDS Prevention.

## References

Bleiber, G., Munoz, M., Ciuffi, A., Meylan, P., Telenti, A., 2001. Individual contributions of mutant protease and reverse transcriptase to viral infectivity, replication, and protein maturation of antiretroviral drug-resistant human immunodeficiency virus type 1. J. Virol. 75, 3291–3300.

Colson, P., Henry, M., Tourres, C., Lozachmeur, D., Gallais, H., Gastaut, J.A., Moreau, J., Tamalet, C., 2004. Polymorphism and drug-selected mutations in the protease gene of human immunodeficiency virus type 2 from patients living in southern France. J. Clin. Microbiol. 42, 570–577.

Cornelissen, M., van den Burg, R., Zorgdrager, F., Lukashov, V., Goudsmit, J., 1997. pol gene diversity of five human immunodeficiency virus type 1 subtypes: evidence for naturally occurring mutations that contribute to drug resistance, limited recombination patterns, and common ancestry for subtypes B and D. J. Virol. 71, 6348–6358.

Croteau, G., Doyon, L., Thibeault, D., McKercher, G., Pilote, L., Lamarre, D., 1997. Impaired fitness of human immunodeficiency virus type 1 variants with high-level resistance to protease inhibitors. J. Virol. 71, 1089–1096.

Doyon, L., Croteau, G., Thibeault, D., Poulin, F., Pilote, L., Lamarre, D., 1996. Second locus involved in human immunodeficiency virus type 1 resistance to protease inhibitors. J. Virol. 70, 3763–3769.

Gatanaga, H., Suzuki, Y., Tsang, H., Yoshimura, K., Kavlick, M.F., Nagashima, K., Gorelick, R.J., Mardy, S., Tang, C., Summers, M.F., Mitsuya, H., 2002. Amino acid substitutions in Gag protein at non-cleavage sites are indispensable for the development of a high multitude of HIV-1 resistance against protease inhibitors. J. Biol. Chem. 277, 5952–5961.

Kosalaraksa, P., Kavlick, M.F., Maroun, V., Le, R., Mitsuya, H., 1999. Comparative fitness of multi-dideoxynucleoside-resistant human immunodeficiency virus type 1 (HIV-1) in an *in vitro* competitive HIV-1 replication assay. J. Virol. 73, 5356–5363.

Martinez-Picado, J., Savara, A.V., Sutton, L., D'Aquila, R.T., 1999. Replicative fitness of protease inhibitor-resistant mutants of human immunodeficiency virus type 1. J. Virol. 73, 3744–3752.

Matsuoka-Aizawa, S., Sato, H., Hachiya, A., Tsuchiya, K., Takebe, Y., Gatanaga, H., Kimura, S., Oka, S., 2003. Isolation and molecular characterization of a nelfinavir (NFV)-resistant human immunodeficiency virus type 1 that exhibits NFV-dependent enhancement of replication. J. Virol. 77, 318–327.

Quinones-Mateu, M.E., Albright, J.L., Mas, A., Soriano, V., Arts, E.J., 1998. Analysis of pol gene heterogeneity, Viral quasispecies, and drug resistance in individuals infected with group O strains of human immunodeficiency virus type 1. J. Virol. 72, 9002–9015.

Tamiya, S., Mardy, S., Kavlick, M.F., Yoshimura, K., Mistuya, H., 2004. Amino acid insertions near Gag cleavage sites restore the otherwise compromised replication of human immunodeficiency virus type 1 variants resistant to protease inhibitors. J. Virol. 78, 12030–12040.

Turner, B.G., Summers, M.F., 1999. Structural biology of HIV. J. Mol. Biol. 285, 1–32.

Zhang, Y.M., Imamichi, H., Imamichi, T., Lane, H.C., Falloon, J., Vasudevachari, M.B., Salzman, N.P., 1997. Drug resistance during indinavir therapy is caused by mutations in the protease gene and in its Gag substrate cleavage sites. J. Virol. 71, 6662–6670.

AIDS RESEARCH AND HUMAN RETROVIRUSES
Volume 22, Number 8, 2006, pp. 744–748


# Urinary $\beta_2$-Microglobulin as a Possible Sensitive Marker for Renal Injury Caused by Tenofovir Disoproxil Fumarate

HIROYUKI GATANAGA, NATSUO TACHIKAWA, YOSHIMI KIKUCHI, KATSUJI TERUYA, IKUMI GENKA, MIWAKO HONDA, JUNKO TANUMA, HIROHISA YAZAKI, AKIHIRO UEDA, SATOSHI KIMURA, and SHINICHI OKA

## ABSTRACT

**Tenofovir disoproxil fumarate (TDF) is renally excreted by a combination of glomerular filtration and active tubular secretion, and its renal safety profiles have been reported based on a limited increase of serum creatinine (sCr) levels. However, renal tubular function has not previously been well monitored. We measured sCr and urinary $\beta_2$-microglobulin (U-$\beta_2$MG) levels cross-sectionally in 70 patients treated with TDF [TDF(+)] and 90 patients on other antiretroviral therapy who had never been exposed to TDF [TDF(−)]. The mean U-$\beta_2$MG was significantly higher in TDF(+) patients than that in TDF(−) patients ($p < 0.0001$), though no statistical difference was detected in their creatinine clearance estimated by using the Cockcroft–Gault equation. Multivariate analysis showed that coadministration of boosted lopinavir (LPV) and patients' body weight were associated with U-$\beta_2$MG levels in TDF(+) patients. U-$\beta_2$MG levels were significantly higher in those who also received boosted LPV [TDF(+)LPV(+)] ($p = 0.0007$), and abnormally high levels were noted in 67.7% of them. Furthermore, in the TDF(+)LPV(+) group, U-$\beta_2$MG levels showed significant negative correlation with patients' body weight ($p = 0.0029$) and abnormal U-$\beta_2$MG was observed in all six patients with body weight less than 55 kg. In four patients, a rapid fall in U-$\beta_2$MG occurred after cessation of TDF. Relative to sCr, U-$\beta_2$MG could be a more sensitive marker of renal tubular injury caused by TDF. Boosted LPV co-administration and low body weight may be risk factors for TDF-induced renal tubular dysfunction, probably because these factors are associated with an increase in TDF concentration.**

## INTRODUCTION

TENOFOVIR DISOPROXIL FUMARATE (TDF) is an orally bioavailable ester prodrug of tenofovir, an acyclic nucleotide analogue with activity against HIV-1, HIV-2, and hepatitis B virus. TDF is administered once daily in HIV treatment and a combination formula with emtricitabine is currently available. TDF does not have high mitochondrial toxicity compared with stavudine[1,2] and it does not induce a systemic hypersensitivity reaction like abacavir.[3] TDF is currently being prescribed for a growing number of HIV-infected patients. One concern regarding use of TDF is its renal toxicity. Several studies showed a limited incidence of renal dysfunction based on the monitoring of serum creatinine (sCr).[4–7] Some cases of TDF-related renal impairment have occurred in patients with underlying systemic or renal diseases.[8–11] However, the majority of the cases of TDF-related renal dysfunction have occurred in patients without any identified risk factor.[12–15] Therefore, careful monitoring of renal function is necessary for the follow-up of TDF-treated patients.

TDF is excreted unchanged in the urine via a combination of glomerular filtration and active tubular secretion.[16] Proximal renal tubular dysfunction and Fanconi's syndrome have been reported to be associated with TDF usage.[10–15,17–19] $\beta_2$-Microglobulin is commonly measured in urine by enzyme-linked immunosorbent assay (ELISA) or latex agglutination assay. It is freely filtered at the glomerulus and is avidly taken up and catabolized by the proximal renal tubules. Therefore, high levels of urinary $\beta_2$-microglobulin (U-$\beta_2$MG) are associated with various pathological conditions involving the proximal renal tubule.[20] In the present study, we compared U-$\beta_2$MG in TDF-treated patients and those on other antiretroviral treatment who had never been exposed to TDF, and assessed the suitability of U-$\beta_2$MG as a sensitive marker of TDF-induced proximal renal

AIDS Clinical Center, International Medical Center of Japan, Tokyo, Japan.

tubular injury compared with creatinine clearance (CrCl) estimated by using the Cockcroft–Gault equation.

## MATERIALS AND METHODS

### *Patients*

Between February 2004 and June 2005, U-$\beta_2$MG was measured cross-sectionally in 70 TDF-treated patients and 90 patients on other antiretroviral treatments who had never been exposed to TDF in the outpatient clinic of the AIDS Clinical Center, International Medical Center of Japan. The U-$\beta_2$MG levels were determined by latex agglutination assay. The normal range of U-$\beta_2$MG was <500 $\mu$g/liter, determined by the analysis of more than 100 healthy volunteers. A signed consent form was obtained from each participant of this study.

### *Statistical analysis*

The sCr concentrations, body weight, CD4 count, HIV-1 viral load measured on the same day with U-$\beta_2$MG, and duration of antiretroviral treatment were also compared. U-$\beta_2$MG was analyzed logarithmically because U-$\beta_2$MG levels change logarithmically in the cases of renal tubular dysfunction and logarithmic analysis compensated the skewed distribution of U-$\beta_2$MG levels in the patients who had never been exposed to TDF [distribution skewness: U-$\beta_2$MG, 2.971; log(U-$\beta_2$MG), 0.412]. CrCl was calculated using the Cockcroft–Gault equation, which estimates CrCl on the basis of sCr level, body weight, and sex of the patient.[21] All data were expressed as mean ± SD. Differences between groups were examined for statistical significance using the Student's *t*-test. Correlations between values were examined using the Pearson's correlation coefficient and the Fisher's *z* transformation. Multivariate least-squares linear regression was used to assess the associations of multiple factors with high U-$\beta_2$MG level. A $p$ value less than 0.05 denoted the presence of statistical significance. Statistical analysis was performed using StatView software (SAS Institute).

## RESULTS

### *Patients*

Between February 2004 and June 2005, U-$\beta_2$MG was measured in 70 TDF-treated patients [TDF(+) group] and 90 patients on other antiretroviral therapy who had never been exposed to TDF [TDF(−) group]. No enrolled patient was taking renal toxic drugs such as ganciclovir or adefovir. In both groups, the HIV-1 RNA loads were less than 400 copies/ml in more than 90% of the patients, suggesting that most patients maintained excellent adherence (Table 1). Most of the analyzed patients were Asian, and around 90% were males. There were no significant differences in age, body weight, CD4 cell count, sCr level, and duration of antiretroviral treatment between TDF(−) and TDF(+) groups.

### *High U-$\beta_2$MG in TDF-treated patients*

U-$\beta_2$MG was measured at least 1 month after the introduction of TDF treatment in TDF(+) patients and the introduction of antiretroviral therapy in TDF(−) patients. TDF(+) patients had significantly higher logarithmic values of U-$\beta_2$MG than TDF(−) patients [2.79 ± 0.85 vs. 2.09 ± 0.43 (log ($\mu$g/liter)), $p < 0.0001$], though there was no significant difference in sCr (0.76 ± 0.18 vs. 0.76 ± 0.15 mg/dl) and in estimated CrCl (114.2 ± 34.3 vs. 120.0 ± 29.8 ml/min) between the two groups (Fig. 1A–C). Thirty of 70 (42.9%) TDF(+) patients had abnormally high U-$\beta_2$MG levels (>500 $\mu$g/liter), although abnormal sCr (>1.1 mg/dl) and abnormal CrCl (<90 ml/min) was observed in only 3 and 11 of them, respectively. There was no significant relation between the duration of TDF treatment and U-$\beta_2$MG values in the TDF(+) group. Six patients had abnormally high U-$\beta_2$MG values within 3 months after the initiation of TDF treatment. In the TDF(−) group, logarithmic U-$\beta_2$MG values showed a normal distribution and abnormally high U-$\beta_2$MG values were observed in only 7 of 90 (7.8%). Eleven of the TDF(−) patients had abnormal CrCl and only one TDF(−) patient with compromised CrCl showed abnormal U-$\beta_2$MG values. There was a significant negative correlation between CrCl

TABLE 1. DEMOGRAPHIC AND CLINICAL CHARACTERISTICS OF ENROLLED PATIENTS

| *Characteristics* | *TDF (−) (n = 90)* | *TDF (+) (n = 70)* |
|---|---|---|
| Sex, no. (%) male | 83 (92.2) | 61 (87.1) |
| Ethnicity, no. (%) | | |
| Asian | 84 (93.3) | 69 (98.6) |
| White | 1 (1.1) | 1 (1.4) |
| African | 3 (3.3) | 0 (0) |
| Half Hispanic half Asian | 2 (2.2) | 0 (0) |
| Age, mean ± SD (years) | 40.4 ± 9.9 | 42.1 ± 12.3 |
| Body weight, mean ± SD (kg) | 64.3 ± 10.2 | 61.6 ± 9.1 |
| CD4 cell count, mean ± SD (cells/mm$^3$) | 461.9 ± 199.8 | 437.4 ± 224.0 |
| HIV-1 RNA load, no. (%) <400 copies/ml | 82 (91.1) | 64 (91.4) |
| Serum creatinine level, mean ± SD (mg/dl) | 0.76 ± 0.15 | 0.76 ± 0.18 |
| Duration of ART,[a] mean ± SD (months) | 40.2 ± 30.7 | 56.6 ± 30.8 |
| Duration of TDF, mean ± SD (months) | Not applicable | 13.0 ± 9.2 |

[a]ART, antiretroviral therapy.

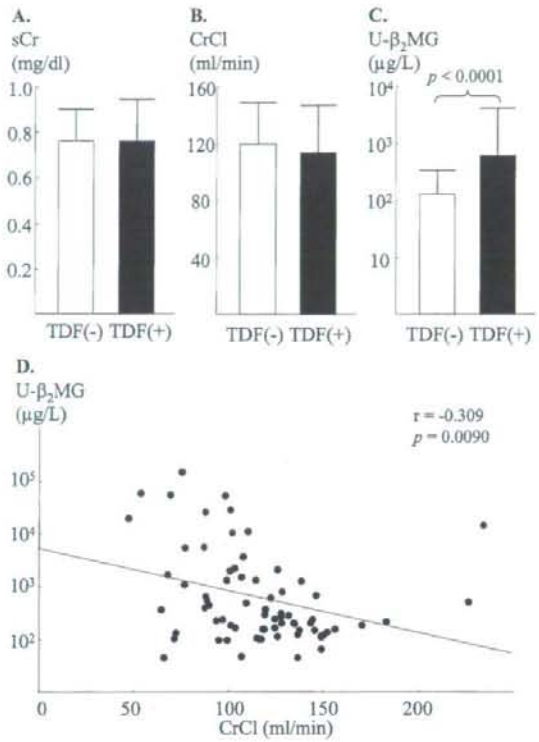


**FIG. 1.** Renal function of 90 TDF(−) and 70 TDF(+) patients. sCr (**A**), CrCl estimated by using Cockcroft–Gault formula (**B**), and U-$\beta_2$MG values (**C**) were compared between 90 TDF(−) (open bar) and 70 TDF(+) (closed bar) patients. Means and SDs are indicated with bars and horizontal lines, respectively. Logarithmic U-$\beta_2$MG values of 90 TDF(+) patients are plotted against CrCl estimated by using the Cockcroft–Gault formula (**D**). The regression line is also shown.

and U-$\beta_2$MG values in the TDF(+) group ($r = -0.309$, $p = 0.0090$) (Fig. 1D) though it was not significant in the TDF(−) group, which suggests renal insufficiency observed in TDF(+) patients was specifically associated with renal tubular damage.

### *Co-administration of boosted LPV as a risk factor*

According to the results of a pharmacokinetic study,[22] TDF exposure was increased by 32% when administered with lopinavir (LPV)/ritonavir (RTV) therapy, compared with TDF monotherapy, which can be considered to accelerate TDF-induced renal injury. In order to analyze the effect of coadministration of RTV-boosted LPV on TDF-induced renal tubular damage, we classified TDF(+) patients into three subgroups by the usage of LPV and RTV, and compared their U-$\beta_2$MG values; those who did not receive LPV or RTV at the time of measurement of U-$\beta_2$MG [TDF(+)LPV(−)RTV(−) group, $n = 29$], those on RTV-boosted protease inhibitor-containing treatment other than LPV [TDF(+)LPV(−)RTV(+) group, $n = 10$], and those on the coadministration of RTV-boosted LPV [TDF(+)LPV(+)RTV(+), $n = 31$] (Fig. 2). There was no significant difference in U-$\beta_2$MG values between the TDF(+)LPV(−)RTV(−) group and the TDF(+)LPV(−)RTV(+) group [2.50 ± 0.78 vs. 2.49 ± 0.37 (log (μg/liter)), $p = 0.966$], suggesting RTV coadministration had little effect on TDF-induced renal injury. However, the U-$\beta_2$MG values of TDF(+)LPV(+)RTV(+) patients [3.17 ± 0.89 (log (μg/liter))] were significantly higher than those in the TDF(+)LPV(−)RTV(−) group ($p = 0.0032$) and those in the TDF(+)LPV(−)RTV(+) group ($p = 0.0257$), and abnormally high levels were noted in 67.7% of TDF(+)LPV(+)RTV(+) patients, indicating that boosted LPV cousage accelerated renal damage by TDF. There were no significant differences in CrCl among the three groups, suggesting that estimated CrCl is less sensitive in detecting TDF-induced renal injury than U-$\beta_2$MG.

### *Low body weight as a risk factor*

When multivariate least-squares linear regression was used to assess the multiple factors including age, body weight, CD4 cell count, and TDF usage, TDF usage was a most significant factor associated with a high U-$\beta_2$MG value (partial regression coefficient = 0.477, $F = 46.7$). In order to identify other risk factors associated with TDF-induced renal injury, the multiple factors including age, body weight, CD4 cell count, duration of TDF treatment, and boosted LPV usage were assessed in TDF(+) patients. Boosted LPV usage had the greatest positive impact on the U-$\beta_2$MG value (partial regression coefficient = 0.394, $F = 12.5$) and patients' body weight had the second greatest impact though it was negative (partial regression coefficient = −0.305, $F = 6.97$) (Table 2). In order to confirm the effect of patients' body weight, U-$\beta_2$MG values were plotted against patients' body weight. In the TDF(+)LPV(+)RTV(+)

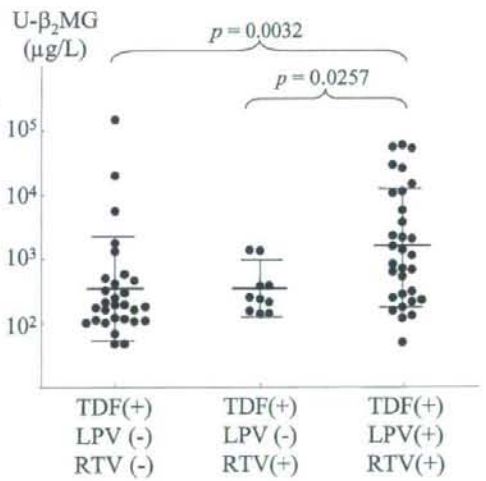


**FIG. 2.** U-$\beta_2$MG levels of TDF-treated patients and LPV and RTV usage. U-$\beta_2$MG values were compared among three subgroups of TDF(+) patients divided by usage of LPV and RTV; 29 TDF(+)LPV(−)RTV(−) patients, 10 TDF(+)LPV(−)RTV(+) patients, and 31 TDF(+)LPV(+)RTV(+) patients. Logarithmic means and SDs are indicated with bold and thin horizontal lines, respectively.

TABLE 2. FACTORS ASSOCIATED WITH U-$\beta_2$MG LEVEL IN TDF-TREATED PATIENTS

| *Factor* | *Partial regression coefficient* | F *value* |
|---|---|---|
| Age (years) | 0.131 | 1.19 |
| Body weight (kg) | −0.305 | 6.97 |
| CD4 cell count (cells/mm$^3$) | −0.237 | 4.03 |
| Duration of TDF (months) | 0.208 | 3.06 |
| LPV usage | 0.394 | 12.5 |

group, U-$\beta_2$MG levels showed significant negative correlation with patients' body weight ($r = -0.511$, $p = 0.0029$) and abnormal U-$\beta_2$MG was observed in all six patients with body weight less than 55 kg (Fig. 3). In the TDF(+)LPV(−) group including TDF(+)LPV(−)RTV(−) patients and TDF(+)LPV(−)RTV(+) patients, patients with lower body weight also tended to have higher U-$\beta_2$MG values, albeit statistically insignificant ($r = -0.151$, $p = 0.361$) (data not shown). When estimated CrCl was plotted against patients' body weight, CrCl showed significant positive correlation with patients' body weight in the TDF(+)LPV(−) group ($r = 0.467$, $p = 0.0024$), and patients with lower body weight also tended to have lower CrCl in the TDF(+)LPV(+) group, albeit statistically insignificant ($r = 0.181$, $p = 0.334$) (data not shown).

### *Rapid fall in U-$\beta_2$MG after cessation of TDF*

Renal injury induced by TDF has been reported to be reversible after cessation of TDF.[10–15,17,18] To confirm this, we examined changes in U-$\beta_2$MG over time after switching from TDF to other antiretroviral agents. During this study period, TDF was switched to other agents in four cases that had abnormally high U-$\beta_2$MG levels before switching the treatment regimen. The U-$\beta_2$MG levels were substantially decreased by 0.86–2.15 log at 5–8 months after switching treatment, and in one case the level was normalized (<500 $\mu$g/liter). Thus, as reported by other investigators,[10–15,17,18] TDF-induced renal injury seems reversible, as evident by changes in U-$\beta_2$MG values.

## DISCUSSION

Renal safety of TDF has been reported based on minimal change in sCr within the normal range during TDF treatment.[4–7] However, we found that 30 of 70 TDF-treated patients had abnormally high U-$\beta_2$MG while only 3 of them had abnormal sCr and only 11 had abnormal CrCl, suggesting that the incidence of renal tubular injury in TDF-treated patients is larger than previously estimated, and that U-$\beta_2$MG can be used as a more sensitive marker of TDF-induced renal injury than sCr.

U-$\beta_2$MG levels have been reported to be reproducible in urine samples collected from the same subjects on multiple occasions,[23] and its measurement is considered a useful tool for noninvasive monitoring of the renal allograft after kidney transplantation.[24] Measurement of urinary protein may be also helpful for monitoring TDF-induced renal injury, though its low specificity might be problematic because not only renal tubular injury but also glomerular damage such as diabetic nephropathy could increase protein excretion in the urine.[20] Furthermore, it was reported that proteinuria is often observed in HIV-infected patients on initial evaluation.[25,26] Therefore, monitoring markers specific to renal tubular injury, such as U-$\beta_2$MG, may be useful for HIV-infected patients treated with TDF.

Our results also showed that boosted LPV-containing treatment and low body weight were associated with high U-$\beta_2$MG in TDF-treated patients. Surprisingly, all TDF- and boosted LPV-treated patients with body weight <55 kg had abnormally high U-$\beta_2$MG. It is possible that boosted LPV usage and low body weight accelerate TDF-induced renal injury by increasing TDF plasma concentrations. In fact, many of the reported cases of TDF-induced renal injury have been in those treated with boosted LPV-containing regimens,[10,12–15,17] and Peyriere *et al.*[10] reported seven cases of TDF-induced renal tubular dysfunction and 6 of them had a low body weight (<60 kg). Patients with low body weight have unusually low sCr levels because creatinine is mainly derived from muscle and lean patients have disproportionately less muscle mass.[27] Therefore, body weight should be taken into consideration when evaluating renal function with sCr values, but this may not be sufficient for full assessment. A simple renal tubular injury is often not associated with an increase in sCr,[20] and mild TDF tubular toxic effects may be missed by the simple and convenient approach of the formula-based estimation of ClCr based on sCr and patient demographics. Thus, sensitive markers, such as U-$\beta_2$MG values, may be of use in monitoring HIV-infected patients during TDF treatment, especially when boosted LPV is coadministered or the patient has low body weight.

Abnormally high U-$\beta_2$MG levels indicate renal tubular injury, though its clinical significance in TDF-treated patients is still unknown. Recently, Gallant *et al.*[5] reported that TDF treat-

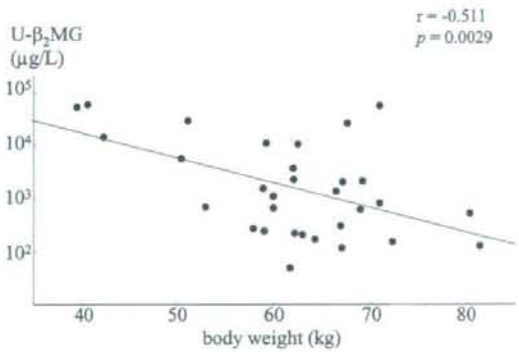


**FIG. 3.** U-$\beta_2$MG values and estimated CrCl in TDF-treated patients. U-$\beta_2$MG values of 31 TDF(+)LPV(+) patients are plotted against patients' body weight. The regression line is also shown.

ment causes a mild decrease of bone density but this was not associated with increased frequency of bone fractures. However, persistence of renal tubular injury in TDF-treated patients may result in significant mineral loss and osteoporosis. It was reported that bone deformities and/or fractures were found in 28% of the pediatric patients with hereditary renal tubular disorders during 10 years of observation.[28] Only a longer trial looking at outcomes of TDF-treated patients with high U-$\beta_2$MG levels would confirm its clinical significance. It is also possible that since most of our patients were Asians, TDF excretion might be different from that reported in other races. Our study is limited by its cross-sectional design and lack of TDF concentrations in the plasma. Prospective and longitudinal analysis of U-$\beta_2$MG value and TDF plasma concentration in a larger cohort is warranted.

## ACKNOWLEDGMENTS

The authors thank Drs. Y. Abe, K. Yokota, and J. Onda for follow-up of the patients. This study was supported in part by a Grant-in-Aid for AIDS research from the Ministry of Health, Labor, and Welfare of Japan (H15-AIDS-001).

## REFERENCES

1. Biesecker G, Karimi S, Desjardins J, *et al.*: Evaluation of mitochondrial DNA content and enzyme levels in tenofovir DF-treated rats, rhesus monkeys and woodchucks. Antiviral Res 2003;58:217–225.
2. Birkus G, Hitchcock MJ, and Cihlar T: Assessment of mitochondrial toxicities in human cells treated with tenofovir: Comparison with other nucleoside reverse transcriptase inhibitor. Antimicrob Agents Chemother 2002;46:716–723.
3. Hewitt RG: Abacavir hypersensitivity reaction. Clin Infect Dis 2002;34:1137–1142.
4. Schooley RT, Ruane P, Myers RA, *et al.*: Tenofovir DF in antiretroviral-experienced patients: Results from a 48-week, randomized, double-blind study. AIDS 2002;16:1257–1263.
5. Gallant JE, Staszewski S, Pozniak AL, *et al.*: Efficacy and safety of tenofovir DF vs stavudine in combination therapy in antiretroviral-naïve patients: A 3-year randomized trial. JAMA 2004;292:191–201.
6. Izzedine H, Hulot JS, Vitteciq D, *et al.*: Long-term renal safety of tenofovir disoproxil fumarate in antiretroviral-naïve HIV-1-infected patients. Data from a double-blind randomized active-controlled multicentre study. Nephrol Dial Transplant 2005;20:743–746.
7. Gallant JE, Parish MA, Keruly JC, and Moore RD: Changes in renal function associated with tenofovir disoproxil fumarate treatment, compared with nucleoside reverse-transcriptase inhibitor treatment. Clin Infect Dis 2005;40:1194–1198.
8. Coca S and Perazella MA: Acute renal failure associated with tenofovir: Evidence of drug-induced nephrotoxicity. Am J Med Sci 2002;324:342–344.
9. Murphy MD, O'Hearn M, Katlama C, *et al.*: Fatal lactic acidosis and acute renal failure after addition of tenofovir to an antiretroviral regimen containing didanosine. Clin Infect Dis 2003;36:1082–1085.
10. Peyriere H, Reynes J, Rouanet I, *et al.*: Renal tubular dysfunction associated with tenofovir therapy: Report of 7 cases. J Acquir Immune Defic Syndr 2004;35:269–273.
11. Izzedine H, Isnard-Bagnis C, Hulot JS, *et al.*: Renal safety of tenofovir in HIV treatment-experienced patients. AIDS 2004;30:1074–1076.
12. Verhelst D, Monge M, Meynard JL, *et al.*: Fanconi syndrome and renal failure induced by tenofovir: A first case report. Am J Kidney Dis 2002;40:1331–1333.
13. Karras A, Lafaurie M, Furco A, *et al.*: Tenofovir-related nephrotoxicity in human immunodeficiency virus-infected patients: Three cases of renal failure, Fanconi syndrome, and nephrogenic diabetes insipidus. Clin Infect Dis 2003;36:1070–1073.
14. Schaaf B, Aries SP, Kramme E, Steinhoff J, and Dalhoff K: Acute renal failure associated with tenofovir treatment in a patient with acquired immunodeficiency syndrome. Clin Infect Dis 2003;37:e41–e43.
15. Gaspar G, Monereo A, Garcia-Reyne A, and de Guzman M: Fanconi syndrome and acute renal failure in a patient treated with tenofovir: A call for caution. AIDS 2004;18:351–352.
16. Cundy KC, Sueoka C, Lynch GR, Griffin L, Lee WA, and Shaw JP: Pharmacokinetics and bioavailability of the anti-human immunodeficiency virus nucleotide analog 9-[(R)-2-(phosphonomethoxy) proxyl]adenine (PMPA) in dogs. Antimicrob Agents Chemother 1998;42:687–690.
17. Rollot F, Nazal EM, Chauvelot-Moachon L, *et al.*: Tenofovir-related Fanconi syndrome with nephrogenic diabetes insipidus in a patient with acquired immunodeficiency syndrome: The role of lopinavir-ritonavir-didanosine. Clin Infect Dis 2003;37:e174–e176.
18. James CW, Steinhaus MC, Szabo S, and Dressier RM: Tenofovir-related nephrotoxicity: Case report and review of the literature. Pharmacotherapy 2004;24:415–418.
19. Mauss S, Berger F and Schmutz G: Antiretroviral therapy with tenofovir is associated with mild renal dysfunction. AIDS 2005;19:93–95.
20. D'Amico G and Bazzi C: Pathophysiology of proteinuria. Kidney Int 2003;63:809–825.
21. Cockcroft DW and Gault MH: Prediction of creatinine clearance from serum creatinine. Nephron 1976;16:31–41.
22. Gilead Sciences: Viread [package insert] 2004.
23. Ikeda M, Ezaki T, Tsukahara T, *et al.*: Reproducibility of urinary cadmium, alpha1-microglobulin, and beta2-microglobulin levels in health screening of the general population. Arch Environ Contam Toxicol 2005;48:135–140.
24. Schaub S, Wilkins JA, Antonovici M, *et al.*: Proteomic-based identification of cleaved urinary beta2-microglobulin as a potential marker for acute tubular injury in renal allografts. Am J Transplant 2005;5:729–738.
25. Szczech LA, Gange SJ, van der Horst C, *et al.*: Predictors of proteinuria and renal failure among women with HIV infection. Kidney Int 2002;61:195–202.
26. Gardner LI, Holmberg SD, Williamson JM, *et al.*: Development of proteinuria or elevated serum creatinine and mortality in HIV-infected women. J Acquir Immune Defic Syndr 2003;32:203–209.
27. Daley BJ, Maliakkal RJ, Dreesen EB, Driscoll DF, and Bistrian BR: Rapid clinical assessment of kidney function based on arm muscle circumference and serum creatinine. Nutrition 1994;10:128–131.
28. Haffner D, Weinfurth A, Manz F, *et al.*: Long-term outcome of paediatric patients with hereditary tubular disorders. Nephron 1999;83:250–260.

Address reprint requests to:
*Hiroyuki Gatanaga*
*AIDS Clinical Center, International Medical Center of Japan*
*1-21-1 Toyama, Shinjuku-ku*
*Tokyo 162-8655, Japan*

*E-mail:* higatana@imcj.acc.go.jp

Cellular Microbiology (2006) 8(10), 1571–1580
doi:10.1111/j.1462-5822.2006.00731.x
First published online 2 May 2006

# Bacterial flagellin inhibits T cell receptor-mediated activation of T cells by inducing suppressor of cytokine signalling-1 (SOCS-1)

**Shu Okugawa,[1] Shintaro Yanagimoto,[1] Kunihisa Tsukada,[1] Takatoshi Kitazawa,[1] Kazuhiko Koike,[1] Satoshi Kimura,[1] Hiroyuki Nagase,[2] Koich Hirai[2] and Yasuo Ota[1]***

*Departments of [1]Infectious Diseases and [2]Bioregulatory Function, Graduate School of Medicine, The University of Tokyo, Tokyo, Japan.*

## Summary

**Flagellin, the structural component of bacterial flagella, is secreted by pathogenic and commensal bacteria, and is recognized by Toll-like receptor (TLR) 5. Flagellin is a common bacterial antigen present on most motile bacteria and is speculated to contribute to the activation of CD4$^+$ T cells in the intestine. However, molecular mechanisms by which flagellin regulate T cell activation remains to be determined. Using Jurkat T cells or human primary T cell, we showed that flagellin stimulation induced tyrosine phosphorylation of TLR5 and activation of both mitogen-activated protein kinases and nuclear factor κB. In addition, stimulation by flagellin did not induce nuclear factor of activated T cells (NFAT) activation, while stimulation via the T cell receptor (TCR) leads to activation of NFAT. However, TCR-mediated NFAT activation and tyrosine phosphorylation of zeta-associated protein 70 (Zap-70) were inhibited in cells pre-stimulated by flagellin. Furthermore, flagellin stimulation induced suppressor of cytokine signalling-1 (SOCS-1), which formed a complex with Zap-70 after stimulation via TCR, and inhibition of SOCS-1 expression by SOCS-1-specific small interfering RNA reinstated TCR-mediated activation of NFAT in cells pre-stimulated with flagellin. These results collectively indicate that bacterial flagellin inhibits TCR-mediated activation of T cells by inducing SOCS-1.**

## Introduction

Toll-like receptors (TLRs) recognize pathogen-associated molecular patterns (PAMPs) and mediate the production of cytokines necessary for the development of effective immunity (Aderem and Ulevitch, 2000; Brightbill and Modlin, 2000; Means *et al.*, 2000; Medzhitov and Janeway, 2000). Flagellin, the structural component of bacterial flagella, is secreted by pathogenic and commensal bacteria, and is recognized by the innate immune system in organisms as diverse as flies, plants and mammals (Samakovlis *et al.*, 1992; Ciacci-Woolwine *et al.*, 1999; Wyant *et al.*, 1999a,b; Gomez-Gomez and Boller, 2000; McDermott *et al.*, 2000; Steiner *et al.*, 2000). Specifically, flagellin is a common bacterial antigen present on most motile bacteria in the intestine (Winstanley and Morgan, 1997). Flagellin is an extremely potent inducer of cytokine and nitric oxide production (McDermott *et al.*, 2000; Steiner *et al.*, 2000; Eaves-Pyles *et al.*, 2001a,b; Gewirtz *et al.*, 2001a,b; Moors *et al.*, 2001; Ogushi *et al.*, 2001; Sierro *et al.*, 2001). Flagellin induces signalling via TLR5 in a variety of cell types including human and murine monocytes, dendritic cells, epithelial cell lines and TLR5-positive intestinal epithelial cells (Gewirtz *et al.*, 2001a; Hayashi *et al.*, 2001; McSorley *et al.*, 2002a; Mizel and Snipes, 2002; Didierlaurent *et al.*, 2004).

As flagellin is ubiquitously present in the intestine and can be transported across intestinal epithelia by some pathogens (Gewirtz *et al.*, 2001b), it may also contribute to the activation of CD4$^+$ T cells in the intestine (McSorley *et al.*, 2002a). Flagellin enhances the clonal expansion of naive CD4$^+$ T cells *in vivo* and induced production of interferon-γ (IFN-γ) *in vitro* (McSorley *et al.*, 2002a). Marked reactivity against flagellin has also been seen in mesenteric and splenic T cell cultures from colitic animals, and flagellin-specific T cells were able to induce colitis when adoptively transferred into immunodeficient animals (Lodes *et al.*, 2004). Flagellin was also found to be a target of CD4$^+$ T cells during murine *Salmonella typhimurium* infection, and antigenic responses against flagellin are protective in *Salmonella* infections in mice (Cookson and Bevan, 1997; McSorley *et al.*, 2000; 2002b). Given the activity of flagellin as a specific ligand for TLR5, these data provide a potentially important link between adaptive and innate immune responses.

T cells express a relatively small number of TLRs, while macrophages or dendritic cells express wide varieties of TLRs. TLR4 is expressed in murine CD3$^+$ T lymphocytes, and more specifically in particular subsets of

Received 13 October, 2005; revised 8 March, 2006; accepted 9 March, 2006. *For correspondence. E-mail yasuota-tky@umin.ac.jp; Tel. (+81) 3 3815 5411; Fax (+81) 3 5800 8805.

γδ T cells (Matsuguchi *et al.*, 2000; Mokuno *et al.*, 2000). Expression of TLR4, TLR5, TLR7 and TLR8 in regulatory T cell subsets have been reported (Caramalho *et al.*, 2003). Recently, it was also reported that effector memory T cells are stimulated by ligands of TLR5, TLR7 and TLR8 (Caron *et al.*, 2005). In addition, exposure to lipopolysaccharide (LPS) markedly increases activity of regulatory T cells and their proliferative response does not require antigen-presenting cells (APC). This response is augmented by T cell receptor (TCR) triggering, and synergizes with IL-2 stimulation (Caramalho *et al.*, 2003). Furthermore, flagellin synergized with TCR-dependent stimulation [anti-CD3 monoclonal antibody (Ab)] upregulates proliferation and cytokine productions in $CD4^+$ T lymphocytes (Caron *et al.*, 2005). However, the effects of flagellin stimulation in these T cells remain to be determined.

Suppressor of cytokine signalling-1 (SOCS-1) is a member of the protein family regulating cytokine signalling pathways via inhibition of key tyrosine phosphorylation events on cytokine receptors and signalling molecules such as JAK family members. SOCS-1 interacts with JAK tyrosine kinases and inhibits kinase activity, thereby suppressing cytokine signal transduction (Yasukawa *et al.*, 2000; Kubo *et al.*, 2003). Furthermore, SOCS-1 expression is rapidly induced by LPS and negatively regulates LPS signalling (Crespo *et al.*, 2000; Crespo *et al.*, 2002). In $SOCS\text{-}1^{-/-}$ mice, innate immunity is strongly enhanced, probably due to hypersensitivity of $SOCS\text{-}1^{-/-}$ mice to IFN-γ (Alexander *et al.*, 1999). SOCS-1 has been implicated in the hypo-responsiveness to cytokines, such as IFN-γ, after exposure of LPS to macrophages (Crespo *et al.*, 2002). SOCS-1-deficient mice are more sensitive to LPS shock than their wild-type littermates, and SOCS-1 overexpression suppresses LPS-induced inhibitory kappa B (I-κB) phosphorylation and NF-κB transcriptional activity (Kinjyo *et al.*, 2002; Nakagawa *et al.*, 2002). However, it was recently reported that SOCS proteins induced by TLR stimulation limit the extent of TLR signalling by inhibiting type I interferon signalling but not the direct NF-κB pathway via TLR (Baetz *et al.*, 2004; Gingras *et al.*, 2004). To our knowledge, no reports on whether SOCS proteins are induced by flagellin stimulation and whether they regulate TLR5-mediated signal transduction cascades have been published.

It was reported that a prior exposure to flagellin results in a subsequent state of flagellin tolerance in Jurkat T cells (Mizel and Snipes, 2002). In this study we examined whether Jurkat T cells or human primary T cells were activated by flagellin and whether pre-treatment of flagellin modulated TCR-mediated activation with particular focus on the role of SOCS-1.

## Results

### *TLR5 surface expression in Jurkat T cells and TLR5 tyrosine phosphorylation by flagellin*

To examine whether Jurkat T cells expressed TLR5 protein on the cell surface, we analysed surface expressions of TLR5 in Jurkat T cells by FACS (Mizel and Snipes, 2002). As shown in Fig. 1A, Jurkat T cells express TLR5 at the cell surface. We next examined whether flagellin itself induced tyrosine phosphorylation of TLR5. As shown in Fig. 1B, flagellin stimulation induced tyrosine phosphorylation of TLR5 within 1 min. To confirm that tyrosine-phosphorylation of TLR5 was specifically induced by flagellin stimulation, we examined whether stimulation

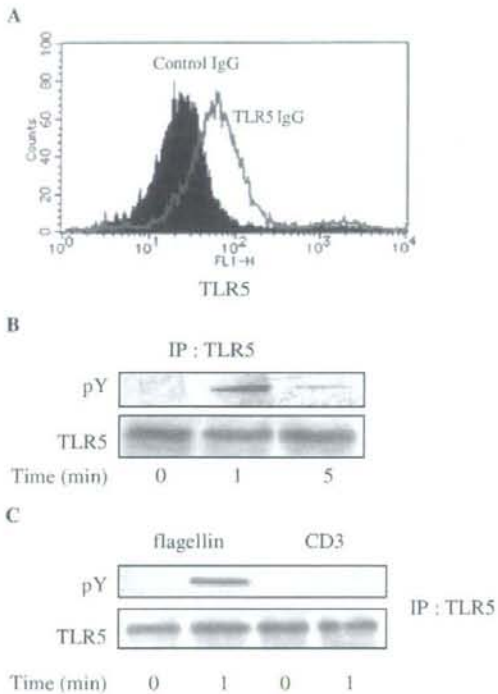


**Fig. 1.** TLR5 is expressed at the cell surface of Jurkat T cells and is tyrosine-phosphorylated by flagellin stimulation.
A. Jurkat T cells were stained with anti-TLR5 antibody (Ab) and FITC-conjugated donkey anti-goat secondary Ab. Cells expressed with TLR5 were examined by FACS analysis.
B. Jurkat T cells were stimulated with 10 ng $ml^{-1}$ flagellin for the indicated times. Cell lysates were immunoprecipitated (IP) with TLR5 Ab and probed with anti-phosphotyrosine Ab, 4G10 (top), or anti-TLR5 (bottom).
C. Jurkat T cells were stimulated with 10 ng $ml^{-1}$ flagellin or 1 μg $ml^{-1}$ anti-CD3 Ab (UCHT1) for 1 min. Cell lysates were immunoprecipitated with TLR5 Ab and probed with anti-phosphotyrosine Ab, 4G10 (top), or anti-TLR5 (bottom).

 

with anit-CD3 Ab induced tyrosine phosphorylation of TLR5. We demonstrated that stimulation with anti-CD3 did not induce tyrosine phosphorylation of TLR5 (Fig. 1C). These results indicate that TLR5 was tyrosine-phosphorylated by flagellin.

### *Flagellin activated NF-κB and mitogen-activated protein kinases, but not NFAT*

As activation of NF-κB and mitogen-activated protein kinases (MAPKs) is the hallmark of TLR-mediated signalling cascades (Muzio *et al.*, 1997; 1998; Yu *et al.*, 2003; Khan *et al.*, 2004), we first examined whether flagellin induced NF-κB activation using a luciferase reporter assay. We demonstrated that the activity of NF-κB was increased in a dose-dependent manner, while *Salmonella* LPS did not activate NF-κB in Jurkat T cells (Fig. 2A). We then examined phosphorylation of MAPKs. Maximal phosphorylation of ERK, c-Jun N-terminal protein kinase (JNK) 1/2 and p38 was observed 15 min after flagellin stimulation (Fig. 2B). These results collectively indicate that flagellin stimulation induced activation of both NF-κB and MAPKs.

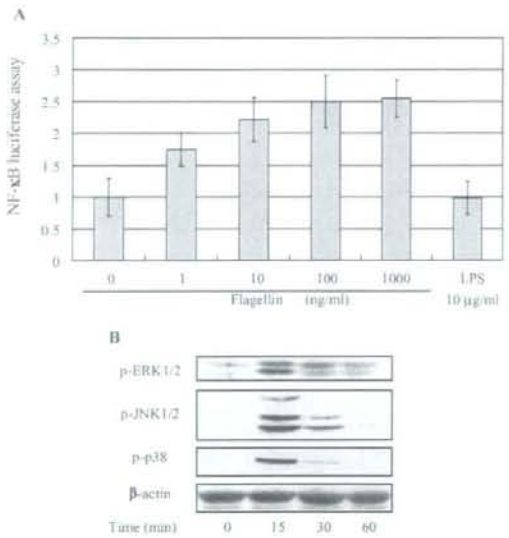


**Fig. 2.** Stimulation by TLR5 induced activation of Jurkat T cells.
A. A total of $1 \times 10^7$ Jurkat T cells were transiently transfected with 30 μg of NF-κB luciferase reporter construct along with 0.03 μg of pRL-TK by electroporation. Twenty-four hours after transfection, the cells were stimulated with the graded concentrations of flagellin or 10 μg ml$^{-1}$ LPS. Six hours after stimulation, the cells were harvested and lysed, and the activities of control *Renilla* luciferase and *Firefly* luciferase (experimental) were measured in triplicate. After normalization according to the *Renilla* luciferase activity, the promoter activity was calculated as fold increase of the control. The data represent the mean ± SD of three independent experiments.
B. Jurkat T cells were stimulated with 10 ng ml$^{-1}$ flagellin for the indicated times. Cell lysates were probed with a phosphospecific Ab for ERK1/2, JNK1/2 and p38, as indicated. Cell lysates were also blotted with β-actin Ab as a loading control.

### *Pre-treatment of flagellin suppressed TCR-mediated activation of NFAT*

We attempted to examine whether pre-treatment of flagellin modulated the TCR-mediated activation of T cells. As NFAT is activated by TCR stimulation (Kane *et al.*, 2000), we analysed TCR-mediated NFAT activities using a luciferase assay in cells pre-treated with flagellin. NFAT activities were significantly suppressed in cells pre-treated with 100 ng ml$^{-1}$ flagellin 6 or 18 h before stimulation with anti-CD3 (Fig. 3A). NFAT activities were also suppressed in a dose-dependent manner in cells pre-treated with graded concentrations of flagellin for 6 h and re-stimulated with anti-CD3 (Fig. 3B). However, TCR-mediated NFAT activities were reinstated 36 h after stimulation with 100 ng ml$^{-1}$ flagellin (Fig. 3C). Furthermore, to exclude the possibility that stimulation with flagellin itself induces NFAT activation in Jurkat T cells, we examined flagellin-induced NFAT activation using a luciferase reporter assay. As shown in Fig. 3D, stimulation with flagellin alone did not activate NFAT, while treatment of PMA plus ionomycin or anti-CD3 Abs activated NFAT. These results suggest that pre-treatment of flagellin inhibited the TCR-mediated activation of T cells, as judged by NFAT activation. However, the inhibitory effect of flagellin on the TCR-mediated activation of T cells was reversible.

### *Flagellin stimulation regulated TCR signalling, but not TCR surface expression*

We then analysed the molecular mechanisms by which pre-treatment of flagellin inhibited the TCR-mediated activation of T cells. First, we examined whether surface expression of TCR was downregulated by pre-treatment with flagellin using a FACS analysis. The levels of TCR expression in cells stimulated with flagellin for 1 or 6 h were almost the same as those in unstimulated cells (Fig. 4A), indicating that expression levels of TCR at the cell surface were unaffected by treatment with flagellin. Next, we compared TCR-mediated intracellular signalling cascade with NFAT activation in cells pre-treated with or without flagellin. Zeta-associated protein 70 (Zap-70) is a tyrosine kinase which is positioned just downstream of TCR in TCR-mediated signalling cascade and is pivotal for TCR-mediated T cell activation, including NFAT activation. Tyrosine phosphorylation of Zap-70 was observed clearly after TCR stimulation in control cells (Fig. 4B). However, pre-treatment with flagellin significantly reduced tyrosine phosphorylation of Zap-70 (Fig. 4B), indicating

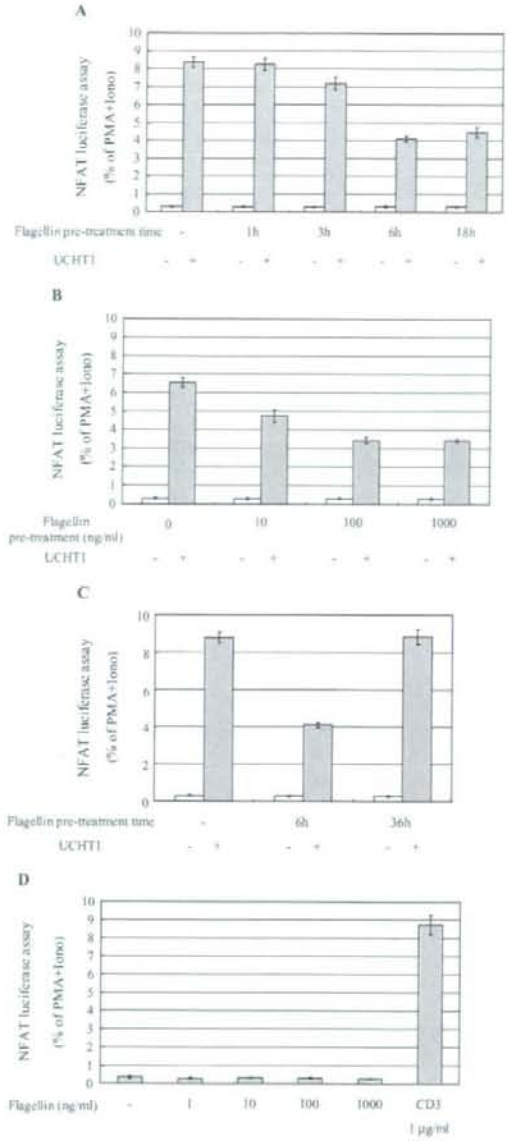


**Fig. 3.** Flagellin pre-treatment inhibited NFAT activation via T cell receptors.
A. Jurkat T cells transfected with NFAT reporter construct and pRL-TK were treated with 100 ng ml$^{-1}$ flagellin for the indicated times prior to anti-CD3 Ab (UCHT1) stimulation. Six hours after stimulation with anti-CD3 Ab, *Renilla* luciferase and *Firefly* luciferase (experimental) were measured in triplicate. After normalization according to the *Renilla* luciferase activity, the promoter activity was expressed as the percentage of response obtained with PMA plus ionomycin. The data represent the mean ± SD of three independent experiments.
B. Jurkat T cells transfected with the NFAT reporter construct and pRL-TK were treated with graded concentrations of flagellin for 6 h. Six hours after stimulation with anti-CD3 Ab, luciferase activities were measured as described in Fig. 3A.
C. Jurkat T cells transfected with NFAT reporter construct and pRL-TK were treated with 100 ng ml$^{-1}$ flagellin for 6 or 36 h prior to anti-CD3 Ab (UCHT1) stimulation. Six hours after stimulation with anti-CD3 Ab, NF-AT luciferase activities were measured as described in (A).
D. Jurkat T cells were transfected with the NFAT reporter construct and pRL-TK as an internal control and were stimulated with graded concentrations of flagellin, 1 μg ml$^{-1}$ anti-CD3 Ab (UCHT1) or PMA plus ionomycin as positive controls. Luciferase activities were examined as described in Fig. 2A.

that flagellin inhibited TCR-mediated signalling events just downstream of TCR.

### *SOCS-1 induced by flagellin negatively regulated TCR-mediated T cell activation*

SOCS proteins are known to be negative regulators in a variety of signalling cascades including LPS or TCR-mediated signalling (Marine *et al.*, 1999; Matsuda *et al.*, 2000; Banerjee *et al.*, 2002; Kinjyo *et al.*, 2002; Nakagawa *et al.*, 2002; Egan *et al.*, 2003). We speculated that SOCS-1 was one of the candidates that negatively regulate TCR-mediated responses in cells pre-treated with flagellin, and examined the level of SOCS-1 expression

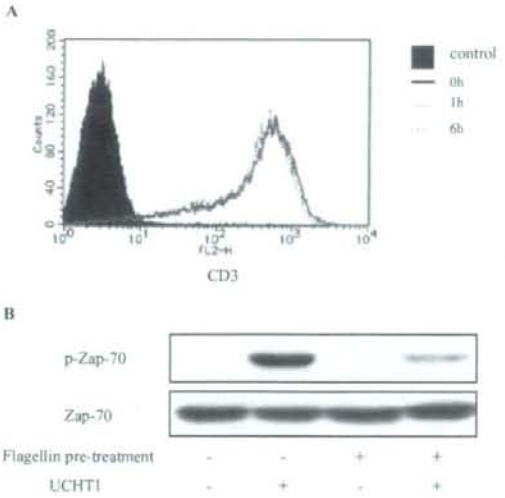


**Fig. 4.** Flagellin pre-treatment had no effect on the surface expression of TCRs, but inhibited TCR-induced tyrosine phosphorylation of Zap-70.
A. Jurkat T cells were stimulated with or without 100 ng ml$^{-1}$ flagellin for the indicated times, and stained with PE-conjugated anti-CD3 Ab. The surface expression of flagellin was analysed by FACS.
B. Jurkat T cells were pre-treated with or without 100 ng ml$^{-1}$ flagellin for 6 h prior to anti-CD3 Ab (UCHT1) stimulation. Then cells were stimulated with 1 μg ml$^{-1}$ anti-CD3 Ab for 1 min. Cell lysates were blotted with phospho-Zap-70 Ab (top) and Zap-70 Ab as a loading control (bottom).

 

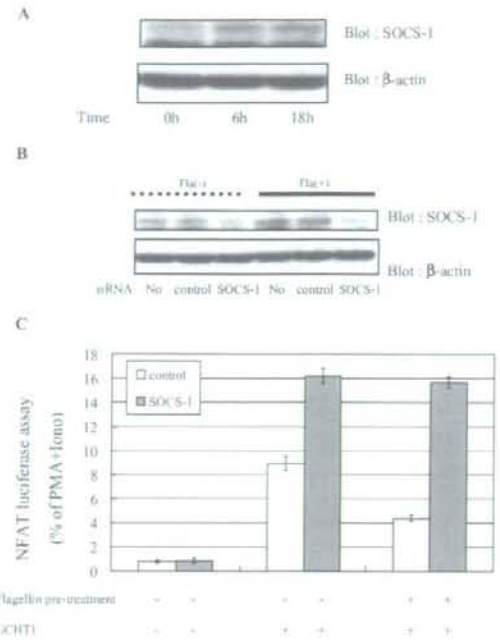


**Fig. 5.** Flagellin stimulation induced SOCS-1, and siRNA specific for SOCS-1 inhibited flagellin-induced SOCS-1 production and reinstated TCR-induced NFAT activation in cells pre-treated with flagellin.
A. Jurkat T cells were stimulated with 100 ng ml$^{-1}$ flagellin for the indicated times. Cell lysates were probed with anti-SOCS-1 Ab. Then the Ab was stripped, and re-probed with a β-actin as a loading control. The data shown are the representative of three experiments.
B. Jurkat T cells were transfected with 10 μg of siRNA specific for SOCS-1, control siRNA or vehicle by electroporation. After incubation for 24 h, cells were stimulated with or without 100 ng ml$^{-1}$ flagellin for 6 h. Cells were lysed and subsequently subjected to SDS-PAGE for Western blotting. The blots were probed with anti-SOCS-1 Ab. Then the Ab was stripped, and the blots were re-probed with a β-actin as a loading control. The data shown are the representative of three experiments.
C. SOCS-1 siRNAs or non-specific control siRNAs were co-transfected with the NFAT luciferase reporter construct and the pRL-TK internal control into Jurkat T cells by electroporation. Then the cells were treated with or without 100 ng ml$^{-1}$ flagellin for 6 h, and stimulated in the presence or absence of anti-CD3 Ab (UCHT1) for 6 h. The luciferase activities were calculated as described in Fig. 3A.

after flagellin stimulation in Jurkat T cells. As shown in Fig. 5A, expression levels of SOCS-1 were very low in unstimulated Jurkat cells, while they were augmented in cells treated with flagellin for 6 or 18 h, indicating that SOCS-1 was induced by flagellin stimulation in Jurkat T cells.

To confirm that flagellin-induced SOCS-1 protein inhibited TCR-mediated NFAT activity, we inhibited expression of SOCS-1 protein by transfection of small interfering RNA (siRNA) specific for SOCS-1. Cells transfected with non-specific siRNA induced the same levels of basal and flagellin-induced SOCS-1 protein as those in control cells (Fig. 5B). However, transfection of siRNA specific for SOCS-1 inhibited expression levels of SOCS-1 protein in both cells pre-treated with or without flagellin (Fig. 5B), indicating that the siRNA inhibited both basal and flagellin-induced SOCS-1 protein expression. We then examined whether inhibition of SOCS-1 protein by siRNA would alter TCR-mediated NFAT activity in cells treated with flagellin. We compared TCR-mediated NFAT luciferase activity between cells transfected with siRNAs specific or non-specific for SOCS-1. As shown in Fig. 5C, NFAT activities were inhibited by flagellin pre-treatment in cells transfected with non-specific SOCS-1 siRNA. However, pre-treatment of siRNA specific for SOCS-1 augmented TCR-mediated activation of NFAT, and flagellin pre-treatment did not inhibit TCR-mediated activation of NFAT (Fig. 5C). These results indicate that flagellin-induced SOCS-1 inhibited TCR-mediated activation of Jurkat T cells.

### *SOCS-1 forms a complex with Zap-70 after TCR stimulation*

To explore the molecular mechanism by which SOCS-1 protein suppressed TCR-mediated NFAT activity, we established a stable cell line that expressed SOCS-1. As shown in Fig. 6A, SOCS-1 was expressed constitutively in these cells. We next compared NFAT luciferase activity and tyrosine phosphorylation of Zap-70 between cells stably transfected with or without SOCS-1. Both TCR-mediated NFAT activity and tyrosine phosphorylation of Zap-70 were inhibited in cells that expressed SOCS-1 constitutively compared with control cells (Fig. 6B and C). In addition, we examined whether SOCS-1 forms a complex with Zap-70 after TCR stimulation. As shown in Fig. 6D, Zap-70 interacted with SOCS-1, and the interaction between Zap-70 and SOCS-1 was dependent on TCR stimulation. These results collectively indicate that SOCS-1 was a negative regulator of TCR-mediated activation of T cells, inhibiting activation of Zap-70 and NFAT.

### *Effects of flagellin stimulation on human primary T cells*

We also determined whether pre-treatment of flagellin inhibited TCR-mediated activation of primary T cells. First, we examined whether flagellin stimulation induced activation of human primary T cells, and analysed flagellin-induced phosphorylation of MAPKs as a representative. As shown in Fig. 7A, three MAPKs, ERK, JNK and p38, were all phosphorylated by flagellin stimulation. Next, we examined whether pre-treatment of flagellin suppressed TCR-mediated phosphorylation of Zap-70. As observed in Jurkat T cells, it was also inhibited in cells pre-treated with flagellin for 6 h before stimulation with anti-CD3 Ab (Fig. 7B). Finally, we showed that SOCS-1 was induced

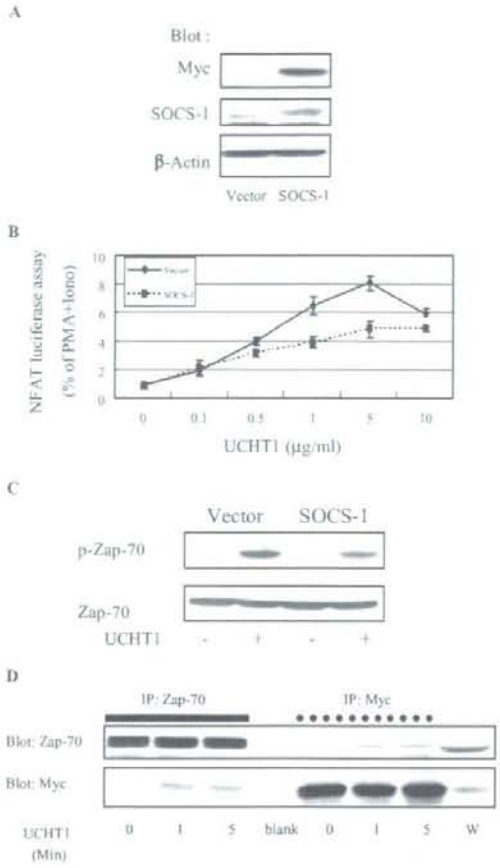


**Fig. 6.** TCR-induced activation of NFAT and tyrosine phosphorylation of Zap-70 was suppressed in cells stably expressed with SOCS-1.
A. To establish a cell line that stably expresses SOCS-1, Jurkat T cells were transfected with pcDNA3-SOCS1-Myc or pcDNA3 (control), and selected in the medium with 600 μg ml$^{-1}$ G418. Protein expression of SOCS-1 in cells stably expressing SOCS-1 or control cells was examined by Western blotting with anti-Myc Ab.
B. Cells stably expressing SOCS-1 or control cells were transfected with the NFAT luciferase reporter construct and pRL-TK by electroporation. Twenty-four hours after transfection cells were stimulated with anti-CD3 Ab (UCHT1). Six hours after stimulation luciferase activities were measured as described in Fig. 3A.
C. Cells stably expressing SOCS-1 or control cells were stimulated with anti-CD3 Ab for 1 min. Then the cell lysates were blotted with a phosphospecific Ab for Zap-70 or Zap-70 Ab as a loading control.
D. Jurkat cells stably expressing SOCS-1 or control cells (E6.1) were stimulated with anti-CD3 Ab for indicated times. Then the cell lysates were immunoprecipitated with anti-Myc or anti-Zap-70 Ab and blotted with anti-Zap-70 or anti-Myc Ab. Whole-cell lysates of Jurkat T cells stably expressing SOCS-1 (W) were used as a control.

by flagellin stimulation in primary T cells (Fig. 7C). These results collectively indicated that pre-treatment of flagellin inhibited the TCR-mediated activation of primary T cells and that flagellin stimulation induced SOCS-1.

## Discussion

We demonstrated for the first time that stimulation by flagellin itself induced tyrosine phosphorylation of TLR5 (Fig. 1B). TLR2 has a YXXM motif whose phosphorylation is important for phosphatidylinositol 3-kinase (PI3-K)

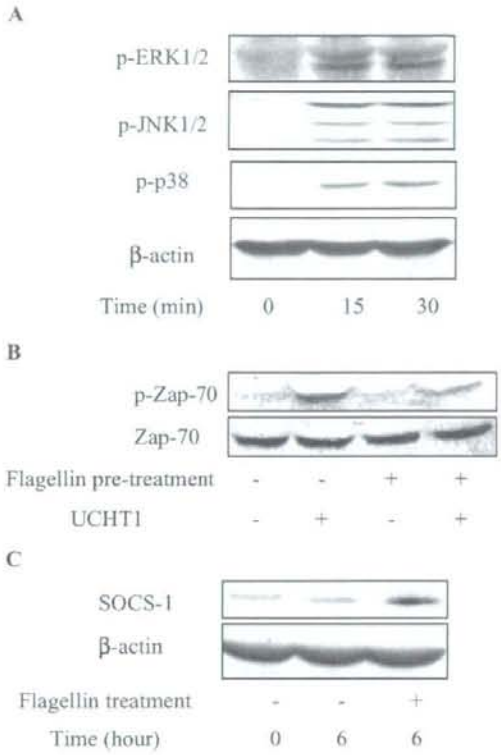


**Fig. 7.** Flagellin stimulation led to phosphorylation of MAPKs, inhibited TCR-mediated activation and induced SOCS-1 in human primary T cells.
A. Human primary T cells were stimulated with 100 ng ml$^{-1}$ flagellin for the indicated times. Cell lysates were probed with a phosphospecific Ab for ERK1/2, JNK1/2 and p38, as indicated. Cell lysates were also blotted with β-actin Ab as a loading control.
B. Primary T cells were pre-treated with or without 100 ng ml$^{-1}$ flagellin for 6 h prior to anti-CD3 Ab (UCHT1) stimulation. Then cells were stimulated with 1 μg ml$^{-1}$ anti-CD3 Ab for 1 min. Cell lysates were blotted with phospho-Zap-70 (top) or Zap-70 Ab as a loading control (bottom).
C. Primary T cells were stimulated with 100 ng ml$^{-1}$ flagellin for the indicated times. Cell lysates were probed with anti-SOCS-1 Ab. Then the Ab was stripped, and re-probed with a β-actin as a loading control. The data shown are the representative of three experiments.

 

association and activation of the TLR2-mediated signal transduction cascade (Arbibe *et al.*, 2000), while phosphorylation of TLR4 is important for activation of NF-κB and IL-8 production (Chen *et al.*, 2003). We speculated that phosphorylation of TLR5 is also important for the activation of the TLR5-mediated signal transduction cascade, although which tyrosine is phosphorylated in TLR5 remains to be determined. In our studies, tyrosine phosphorylation of TLR5 indicates that flagellin activated the cells through TLR5. As Jurkat T cells do not express TLR4 and were not activated by LPS in our study (data not shown), activation was carried out by flagellin via TLR5, not by impure ingredients such as LPS. Flagellin stimulation induced activation of both MAPKs (Figs 2A and 7A) and NF-κB (Fig. 2B), which are important for the TLR-mediated signal transduction cascade in T cells. Although stimulation by flagellin is involved in cytokine production in macrophages or dendritic cells, we did not detect flagellin-induced production of cytokines, such as TNF-α, IL-1β, IL-6 and IL-2, in Jurkat T cells (data not shown), indicating that the role of flagellin-induced activation of T cells may be different from that of macrophages or dendritic cells.

Stimulation by flagellin itself did not induce NFAT activation in T cells, while stimulation via TCR lead to the activation of NFAT (Fig. 3C). However, TCR-mediated NFAT activation was inhibited in cells pre-stimulated by flagellin (Fig. 3A). We speculated that flagellin stimulation might downregulate cell surface expression of TCR or inhibit molecules in the signal transduction cascade downstream of TCR. However, pre-treatment of flagellin had no effect on the expression of TCR on the cell surface (Fig. 4A). Interestingly, pre-treatment of flagellin inhibited tyrosine phosphorylation of Zap-70 which is a crucial tyrosine kinase in TCR-mediated activation of T cells (Figs 4B and 7B), thus indicating that pre-treatment of flagellin interfered with activation of the molecules just downstream of TCR in TCR-mediated signal transduction cascade. The inhibitory effect of flagellin on Zap-70 phosphorylation appears to be greater than that on NFAT-mediated gene expression. One possibility is that NFAT gene expression might be regulated in part by the molecules that is not located downstream of Zap-70 in the TCR-mediated signal cascade and that is not affected by flagellin pre-stimulation. Another possibility is that the difference might be due to using different assay systems, Western blotting and luciferase assay.

Proteins in SOCS family inhibit signal transduction cascades mainly through cytokine receptors (Elliott and Johnston, 2004), and negatively regulate TCR-mediated activation of T cells (Marine *et al.*, 1999; Matsuda *et al.*, 2000; Egan *et al.*, 2003). For example, SOCS-3 inhibits TCR-mediated NFAT activation by binding to calcineurin (Banerjee *et al.*, 2002). In addition, SOCS-1 is induced by LPS stimulation (Kinjyo *et al.*, 2002; Nakagawa *et al.*, 2002). As T cells over-respond to stimulation through TCR in SOCS-1-deficient mice (Egan *et al.*, 2003), and activation of NFAT is suppressed by binding Splenic Tyrosine Kinase (Syk) to SOCS-1 in HEK293 cells that express Syk and SOCS-1 (Matsuda *et al.*, 2000), we speculated that SOCS-1 might be involved in suppression of TCR-mediated activation of NFAT in cells pre-stimulated with flagellin. We showed that SOCS-1 is induced by flagellin stimulation (Figs 5A and 7C). Furthermore, inhibiting SOCS-1 expression by SOCS-1-specific siRNA reinstates TCR-mediated activation of NFAT in cells pre-stimulated with flagellin (Fig. 5C). These results collectively indicated that SOCS-1 inhibited TCR-mediated NFAT activation directly or indirectly in cells pre-treated with flagellin. In addition, TCR-mediated activation of NFAT was also inhibited in cells stably expressing SOCS-1 and pre-stimulated with flagellin (Fig. 6B). However, the level of inhibition of NFAT-mediated gene expression was lower in cells stably expressing SOCS-1 than that in control cells stimulated with flagellin. We speculated that NFAT-mediated gene expression might be inhibited in part by molecules other than SOCS-1. SOCS-1 is associated with activated Jak family kinases through its SH2 domain in interferon or cytokine receptor signalling cascades, and negatively regulates their signal transduction cascades (Elliott and Johnston, 2004). As co-stimulation by interferons or cytokines also augments TCR-mediated T cell activation (Romano *et al.*, 1996; Zella *et al.*, 2000), we cannot deny the possibility that SOCS-1 might inhibit action of interferons or cytokines, and thus negatively regulate T cell activation via TCR. However, we demonstrated that activation via TCR leads to a complex forming between SOCS-1 and Zap-70 upon induction of the TCR-mediated signalling cascade in Jurkat T cells (Fig. 6D). We also observed that the degrees of TCR-mediated NFAT activation in Jurkat T cells stably expressing SOCS-1 were significantly lower than those in control Jurkat T cells when they were cultured in the absence of serum overnight (data not shown). Thus, we speculated that SOCS-1 induced by flagellin stimulation directly inhibited TCR-mediated NFAT activation, probably by interfering with activation of Zap-70.

In this article, we report that pre-stimulation by flagellin inhibited TCR-mediated activation in T cells. Our study is important for understanding the molecular mechanisms of host defences mediated by T cells. Why are T cells that are stimulated with flagellin made refractory to TCR-mediated activation? We speculate that inhibition of TCR-mediated activation by flagellin might represent a host mechanism aimed at limiting inflammatory damage on activation of the immune system by flagellated bacteria because excessive inflammatory responses is potentially harmful to the host and may lead to microcirculatory dysfunction, causing tissue damage and septic shock. Thus,

 

our study may lead to the development of improved treatments for inflammatory responses to flagellated bacteria that may cause sepsis.

## Experimental procedures

### *Purification of human primary T cells*

Peripheral blood mononuclear cells (PBMC) were isolated from human healthy volunteers by a standard density gradient centrifugation on Ficoll-Paque (MP Biomedicals, OH), and T cells were subsequently purified by negative selection with magnetic beads according to the manufacturer's instructions (StemCell Technologies, Canada). Purity of T cells were about 95–97% measured by flow cytometry using Phycoerythrin (PE)-conjugated anti-CD3 mouse monoclonal Ab.

### *Cell line, reagents and antibodies*

The human acute leukaemia T cell line, Jurkat E6.1 (American Type Culture Collection, Manassas, VA) and purified T cells were maintained in RPMI 1640 supplemented with 2 mM glutamine (Sigma, St Louis, MO), 100 units $ml^{-1}$ penicillin, 100 $\mu g\ ml^{-1}$ streptomycin (ICN, Aurora, OH) and 10% fetal bovine serum (Sanko, Japan). *Salmonella muenchen* flagellin was purchased from Calbiochem (San Diego, CA). *Salmonella typhosa* LPS, phorbol myristate acetate (PMA), ionomycin calcium salt were purchased from Sigma. The following Abs were used in the experiments: anti-TLR5 goat Ab, c-Myc mouse monoclonal Ab (9E10), fluorescein isothiocyanate (FITC)-conjugated anti-goat donkey Ab, control goat IgG Ab and PE-conjugated mouse IgG Ab (Santa Cruz Biotechnology), anti-phosphotyrosine mouse monoclonal Ab (4G10; Upstate, Lake Placid, NY), anti-β-actin mouse monoclonal Ab (Abcam, Cambridge, UK), anti-phosphorylated JNK1/2 Ab and anti-phosphorylated p38 Ab (Cell Signalling Berverly, MA), anti-CD3 mouse monoclonal Ab and PE-conjugated anti-CD3 mouse monoclonal Ab (Pharmingen, San Diego, CA), horseradish peroxidase (HRP)-conjugated anti-rabbit IgG (Dako, Denmark), anti-SOCS-1 Ab (Zymed Laboratories, South San Francisco, CA).

### *Flow cytometric analysis*

Flow cytometric analysis was performed essentially as described previously (Nagase *et al.*, 2000). Briefly, cells were incubated with anti-TLR5, followed by staining with FITC-conjugated anti-goat donkey Ab, or cells were stained with PE-conjugated anti-CD3 mouse monoclonal Ab. Expression of TLR5 or CD3 was analysed by using a BD LSR (BD biosciences, Franklin Lakes, NJ).

### *Establishing a stable cell line that expresses SOCS-1*

To establish a cell line that stably expresses SOCS-1, $1 \times 10^7$ Jurkat T cells were transfected by electroporation with 50 $\mu g$ of pcDNA3MycSOCS-1 construct (kindly provided by Dr A. Yoshimura), using a Gene Pulser II (Bio-Rad) set at 290 V, 970 $\mu F$. Cells that expressed SOCS-1 were selected by incubation in media containing 600 $\mu g\ ml^{-1}$ G418 (Life Technologies, Gaithersburg, MD) and cloned by a standard limiting dilution method. Protein expression of SOCS-1 in cells was examined by Western blotting.

### *Transfection and dual luciferase reporter assay*

Transfection and luciferase reporter assays were performed essentially as previously reported (Nakayama *et al.*, 2003). Briefly, $1 \times 10^7$ Jurkat T cells were co-transfected by electroporation with 30 $\mu g$ of NFAT luciferase reporter plasmid (kindly provided by Drs B. Barbara and R.L. Wange) or 30 $\mu g$ of pNF-κB luciferase reporter plasmid (Stratagene, La Jolla, CA), and 0.03 $\mu g$ of *Renilla* luciferase reporter vector pRL-TK (Promega, Madison, WI). Twenty-four hours after transfection, cells were either left untreated or were incubated with anti-CD3 monoclonal Ab UCHT1, flagellin, LPS or PMA (30 $ng\ ml^{-1}$) plus ionomycin (1.5 $\mu M$). Six hours after stimulation, cells were lysed, and luciferase activities were measured by a dual luciferase reporter assay system (Promega, Madison, WI). Data were obtained by calculating the ratio of *Firefly* luciferase activity (experimental) and *Renilla* luciferase activity (control) and were expressed as the relative luciferase activities representing the mean ± SD of triplicate experiments. NFAT luciferase activities were reported as the percentage of those produced by stimulation with PMA and ionomycin.

### *Immunoprecipitation and immunoblotting*

Immunoprecipitation and Western blotting were performed as previously described (Okugawa *et al.*, 2003). Briefly, cells were lysed in ice-cold NP-40 lysis buffer containing 1% NP-40, 25 mM Tris-HCl (pH 7.5), 150 mM sodium chloride, 1 mM ethylenediaminetetraacetic acid (EDTA), 5 mM sodium fluoride, 1 mM sodium orthovanadate, 1 mM leupeptin and 1 mM phenylmethylsulphonyl fluoride. For immunoprecipitation studies, cell lysates were mixed with the indicated Abs for 1 h. Cell lysates were then mixed with protein G-coupled Sepharose beads and rotated for 1 h at 4°C. After the beads were washed three times with ice-cold NP-40 lysis buffer, the precipitated proteins were boiled for 5 min and eluted with sodium dodecyl sulphate-polyacrylamide gel electrophoresis (SDS-PAGE) sample buffer. For the precipitation of total-cell lysates, cells were lysed directly by the addition of SDS-PAGE sample buffer containing 2-mercaptoethanol.

Immunoprecipitated proteins and cell lysates were separated by SDS-PAGE under reducing conditions and were electrically transferred to a polyvinylidene difluoride membrane. The membrane was blocked for 1 h at room temperature with 1% bovine serum albumin in TBS (Tris-buffered saline) buffer. The membrane was then incubated with the indicated Ab and the reactive bands were visualized with an enhanced chemiluminescence (ECL) detection system (Amersham-Pharmacia Biotech, UK).

### *Constructions and transfection of siRNA*

The constructions of siRNA molecules specific for SOCS-1 were evaluated by B-Bridge International (Sunnyvale, CA). The oligonucleotide sequences used in the experiments were as follows: 5′-CggAACTgCTTTTTCgCCCTT-3′. SOCS-1-specific and negative control RNAs were obtained from Dharmacon (CO). siRNAs specific for SOCS-1 or control RNAs were transfected into Jurkat T cells by electroporation.

**Acknowledgements**

We are grateful to M. Kataoka for preparation of the manuscripts. This work was supported in part by a grant-in-aid for scientific research to S.O. and Y.O. from the Japanese Ministry of Education, Culture, Sports, Science and Technology.

**References**

Aderem, A., and Ulevitch, R.J. (2000) Toll-like receptors in the induction of the innate immune response. *Nature* **406:** 782–787.

Alexander, W.S., Starr, R., Fenner, J.E., Scott, C.L., Handman, E., Sprigg, N.S., *et al.* (1999) SOCS1 is a critical inhibitor of interferon gamma signaling and prevents the potentially fatal neonatal actions of this cytokine. *Cell* **98:** 597–608.

Arbibe, L., Mira, J.P., Teusch, N., Kline, L., Guha, M., Mackman, N., *et al.* (2000) Toll-like receptor 2-mediated NF-kappa B activation requires a Rac1-dependent pathway. *Nat Immunol* **1:** 533–540.

Baetz, A., Frey, M., Heeg, K., and Dalpke, A.H. (2004) Suppressor of cytokine signaling (SOCS) proteins indirectly regulate toll-like receptor signaling in innate immune cells. *J Biol Chem* **279:** 54708–54715.

Banerjee, A., Banks, A.S., Nawijn, M.C., Chen, X.P., and Rothman, P.B. (2002) Cutting edge: suppressor of cytokine signaling 3 inhibits activation of NFATp. *J Immunol* **168:** 4277–4281.

Brightbill, H.D., and Modlin, R.L. (2000) Toll-like receptors: molecular mechanisms of the mammalian immune response. *Immunology* **101:** 1–10.

Caramalho, I., Lopes-Carvalho, T., Ostler, D., Zelenay, S., Haury, M., and Demengeot, J. (2003) Regulatory T cells selectively express toll-like receptors and are activated by lipopolysaccharide. *J Exp Med* **197:** 403–411.

Caron, G., Duluc, D., Fremaux, I., Jeannin, P., David, C., Gascan, H., and Delneste, Y. (2005) Direct stimulation of human T cells via TLR5 and TLR7/8: flagellin and R-848 up-regulate proliferation and IFN-gamma production by memory CD4+ T cells. *J Immunol* **175:** 1551–1557.

Chen, L.Y., Zuraw, B.L., Zhao, M., Liu, F.T., Huang, S., and Pan, Z.K. (2003) Involvement of protein tyrosine kinase in Toll-like receptor 4-mediated NF-kappa B activation in human peripheral blood monocytes. *Am J Physiol Lung Cell Mol Physiol* **284:** L607–L613.

Ciacci-Woolwine, F., McDermott, P.F., and Mizel, S.B. (1999) Induction of cytokine synthesis by flagella from gram-negative bacteria may be dependent on the activation or differentiation state of human monocytes. *Infect Immun* **67:** 5176–5185.

Cookson, B.T., and Bevan, M.J. (1997) Identification of a natural T cell epitope presented by *Salmonella*-infected macrophages and recognized by T cells from orally immunized mice. *J Immunol* **158:** 4310–4319.

Crespo, A., Filla, M.B., Russell, S.W., and Murphy, W.J. (2000) Indirect induction of suppressor of cytokine signalling-1 in macrophages stimulated with bacterial lipopolysaccharide: partial role of autocrine/paracrine interferon-alpha/beta. *Biochem J* **349:** 99–104.

Crespo, A., Filla, M.B., and Murphy, W.J. (2002) Low responsiveness to IFN-gamma, after pretreatment of mouse macrophages with lipopolysaccharides, develops via diverse regulatory pathways. *Eur J Immunol* **32:** 710–719.

Didierlaurent, A., Ferrero, I., Otten, L.A., Dubois, B., Reinhardt, M., Carlsen, H., *et al.* (2004) Flagellin promotes myeloid differentiation factor 88-dependent development of Th2-type response. *J Immunol* **172:** 6922–6930.

Eaves-Pyles, T., Murthy, K., Liaudet, L., Virag, L., Ross, G., Soriano, F.G., *et al.* (2001a) Flagellin, a novel mediator of *Salmonella*-induced epithelial activation and systemic inflammation: I kappa B alpha degradation, induction of nitric oxide synthase, induction of proinflammatory mediators, and cardiovascular dysfunction. *J Immunol* **166:** 1248–1260.

Eaves-Pyles, T.D., Wong, H.R., Odoms, K., and Pyles, R.B. (2001b) *Salmonella* flagellin-dependent proinflammatory responses are localized to the conserved amino and carboxyl regions of the protein. *J Immunol* **167:** 7009–7016.

Egan, P.J., Lawlor, K.E., Alexander, W.S., and Wicks, I.P. (2003) Suppressor of cytokine signaling-1 regulates acute inflammatory arthritis and T cell activation. *J Clin Invest* **111:** 915–924.

Elliott, J., and Johnston, J.A. (2004) SOCS: role in inflammation, allergy and homeostasis. *Trends Immunol* **25:** 434–440.

Gewirtz, A.T., Navas, T.A., Lyons, S., Godowski, P.J., and Madara, J.L. (2001a) Cutting edge: bacterial flagellin activates basolaterally expressed TLR5 to induce epithelial proinflammatory gene expression. *J Immunol* **167:** 1882–1885.

Gewirtz, A.T., Simon, P.O., Jr, Schmitt, C.K., Taylor, L.J., Hagedorn, C.H., O'Brien, A.D., *et al.* (2001b) *Salmonella typhimurium* translocates flagellin across intestinal epithelia, inducing a proinflammatory response. *J Clin Invest* **107:** 99–109.

Gingras, S., Parganas, E., de Pauw, A., Ihle, J.N., and Murray, P.J. (2004) Re-examination of the role of suppressor of cytokine signaling 1 (SOCS1) in the regulation of toll-like receptor signaling. *J Biol Chem* **279:** 54702–54707.

Gomez-Gomez, L., and Boller, T. (2000) FLS2: an LRR receptor-like kinase involved in the perception of the bacterial elicitor flagellin in *Arabidopsis*. *Mol Cell* **5:** 1003–1011.

Hayashi, F., Smith, K.D., Ozinsky, A., Hawn, T.R., Yi, E.C., Goodlett, D.R., *et al.* (2001) The innate immune response to bacterial flagellin is mediated by Toll-like receptor 5. *Nature* **410:** 1099–1103.

Kane, L.P., Lin, J., and Weiss, A. (2000) Signal transduction by the TCR for antigen. *Curr Opin Immunol* **12:** 242–249.

Khan, M.A., Kang, J., and Steiner, T.S. (2004) Enteroaggregative *Escherichia coli* flagellin-induced interleukin-8 secretion requires Toll-like receptor 5-dependent p38 MAP kinase activation. *Immunology* **112:** 651–660.

Kinjyo, I., Hanada, T., Inagaki-Ohara, K., Mori, H., Aki, D., Ohishi, M., *et al.* (2002) SOCS1/JAB is a negative regulator of LPS-induced macrophage activation. *Immunity* **17:** 583–591.

Kubo, M., Hanada, T., and Yoshimura, A. (2003) Suppressors of cytokine signaling and immunity. *Nat Immunol* **4:** 1169–1176.

Lodes, M.J., Cong, Y., Elson, C.O., Mohamath, R., Landers, C.J., Targan, S.R., *et al.* (2004) Bacterial flagellin is a dominant antigen in Crohn's disease. *J Clin Invest* **113:** 1296–1306.

McDermott, P.F., Ciacci-Woolwine, F., Snipes, J.A., and Mizel, S.B. (2000) High-affinity interaction between gram-

 